Cross Sections for Electron Collisions with Methane

Mi-Young Song, Jung-Sik Yoon, Hyuck Cho, Yukikazu Itikawa, Grzegorz P. Karwasz, Viatcheslav Kokoouline , Yoshiharu Nakamura, and Jonathan Tennyson

Citation: Journal of Physical and Chemical Reference Data **44**, 023101 (2015); doi: 10.1063/1.4918630
View online: http://dx.doi.org/10.1063/1.4918630
View Table of Contents: http://scitation.aip.org/content/aip/journal/jpcrd/44/2?ver=pdfcov
Published by the AIP Publishing

Cross Sections for Electron Collisions with Methane

Mi-Young Song[a] **and Jung-Sik Yoon**
Plasma Technology Research Center, National Fusion Research Institute, 814-2 Osikdo-dong, Gunsan, Jeollabuk-do 573-540, South Korea

Hyuck Cho
Department of Physics, Chungnam National University, Daejeon 305-764, South Korea

Yukikazu Itikawa
Institute of Space and Astronautical Science, Sagamihara 252-5210, Japan

Grzegorz P. Karwasz
Faculty of Physics, Astronomy and Applied Informatics, University Nicolaus Copernicus, Grudziadzka 5, 87100 Toruń, Poland

Viatcheslav Kokoouline
Department of Physics, University of Central Florida, Orlando, Florida 32816, USA

Yoshiharu Nakamura
6-1-5-201 Miyazaki, Miyamae, Kawasaki 216-0033, Japan

Jonathan Tennyson
Department of Physics and Astronomy, University College London, Gower Street, London WC1E 6BT, United Kingdom

(Received 18 December 2014; accepted 8 April 2015; published online 28 May 2015)

Cross section data are compiled from the literature for electron collisions with methane (CH_4) molecules. Cross sections are collected and reviewed for total scattering, elastic scattering, momentum transfer, excitations of rotational and vibrational states, dissociation, ionization, and dissociative attachment. The data derived from swarm experiments are also considered. For each of these processes, the recommended values of the cross sections are presented. The literature has been surveyed through early 2014. © *2015 AIP Publishing LLC.* [http://dx.doi.org/10.1063/1.4918630]

Key words: attachment; dissociation; electron collisions; evaluation; ionization; total cross sections.

CONTENTS

List of Tables

[a]Author to whom correspondence should be addressed; electronic mail. mysong@nfri.re.kr.

List of Figures

1. Introduction

Methane (CH_4) is the simplest hydrocarbon molecule and has attracted significant interest as a target for low-energy electron collision studies. It has many technological and atmospheric applications as well as a fundamental importance as one of the testing grounds for collision theories. The molecule

TABLE 1. Vibrational modes and excitation energies for $^{12}CH_4$ (Ref. 2)

	Mode	Energy (eV)
ν_1	Symmetric stretching	0.362
ν_2	Twisting	0.190
ν_3	Asymmetric stretching	0.374
ν_4	Scissoring	0.162

has a nearly isotropic electron–molecule interaction potential and serves as a model system in the development of electron–polyatomic molecule scattering theory.[1] The methane molecule is relatively stable and the strength of the H–CH_3 bond is 4.51 eV. The molecule is nonpolar and has electronic polarizability of 2.885×10^{-40} F m^2. It has four vibrational excitation modes[2] as given in Table 1. Electron collisions with methane are especially important in plasmas. Methane plays a dominant role in the edge plasma region of high temperature plasma apparatus such as a tokamak. Perhaps, the most difficult problem when designing a fusion reactor is that of erosion of the plasma facing surfaces.[3] When a tokamak is operated at high density, so that the diverter plasma temperature is low, the dominant source of carbon impurity in the plasma can be from methane production. The effect of chemical erosion on the tokamak plasma can only be modeled if the transport of the produced methane and its daughter products can be followed in the plasma edge. It is clear that details of atomic and molecular physics are crucial to the understanding of diverter operation in this regime.[3] Other than tokamak applications, methane plasmas are used for carbon coating of metals, deposition of diamond-like thin films, and other technical processes. Studies of plasma-enhanced combustion have also focused extensively on methane plasmas.[4,5] Methane is a major component of the atmospheres of the outer planets and satellites. In particular, atomic processes involving methane play a crucial role in the upper-atmosphere of Titan.[6]

The accuracy for the measured cross section data for processes involving ground state species is good to 5%–10% for some reactions. However, there are reactions for which there are no measurements available at all, and clearly, this situation has to be improved. Even for the available data, there are big discrepancies existing for some reactions, so it is desirable to have an evaluated data set. Reflecting the importance of methane for various applications, a number of cross section compilations have been published.[7–11] These papers report extensive sets of cross sections available at the time of writing. However, the cited publications are all more than ten years old, and a considerable number of new cross sections are available now. The aim of the present paper is to re-examine the available cross sections for methane and to establish an up-to-date set of recommended cross sections. In this paper, we compiled and reviewed the reported data, up to early 2014, of the various cross sections for electron scattering from methane; we suggest recommended cross sections for the different scattering processes.

2. Total Scattering Cross Section

For the total cross section (TCS), our recommendations are based on several experiments shown in Table 2 with partially overlapping energy ranges. Absolute measurements using the transmission method were selected: the total cross section, σ, is determined from the electron beam attenuation using Beer–Lambert's law,

$$I = I_0 \exp(-\sigma N l), \quad (1)$$

where I is the electron current in the presence of gas in the scattering cell, I_0 is the current without gas in the scattering cell, N is the target density, and l is the gas cell length (in some experiment the "effective" length of the scattering cell was used).

The experiments chosen were performed using the following complementary methods:

- time-of-flight (Ferch *et al.*,[12] Lohmann and Buckman,[13] and Jones[14]),
- linear transmission with electrostatic electron-beam selection (Szmytkowski from Zecca *et al.*,[15] Kanik *et al.*,[18] and Nishimura and Sakae[17]),
- linear transmission with retarding-field analyzer at the detector (García and Manero[20] and Ariyasinghe *et al.*,[19])
- curved geometry with magnetic guiding and/or beam selection (Dababneh *et al.*,[16] Zecca *et al.*[15]).

The chosen experimental data are compared with recommended values in Fig. 1. Generally, the agreement between all sets of chosen data is very good, i.e., within ±5%. The data from some experiments deviate downwards by more than few per cent from the recommended set near their upper energy limits. This is the case for the TCS of Ferch *et al.*[12] at 10 eV (~7%), Nishimura and Sakae[17] above 100 eV (~12% at 500 eV), and Zecca *et al.*[15] (~30% at 4000 eV). The reason for these discrepancies is the rising angular resolution error in the high-energy limits of the apparatuses. In the experiment of Zecca *et al.*,[15] the additional error is explainable by the lack of a retarding-field analyzer at the detector, which means that inelastically scattered electrons (in ionization and/or electronic excitation events) are counted as non-scattered. The recommended values shown in Table 3 were obtained as weighted average values out of all experiments considered, with weight equal to the total experimental errors declared. The high-energy limits of the experiments—above 100 eV by Nishimura and Sakae[17] and above 1000 eV by Zecca *et al.*[15] were excluded from the averaging procedures. As this procedure is identical to the one used in the Landolt–Börnstein review,[24] the set of data is also identical in the energy range 0.1–1000 eV. However, at low energies, in the range of 0–0.1 eV, the TCS (which is equal to the integral elastic cross sections) is based on the modified effective range model by Fedus and Karwasz[25] obtained from elastic differential measurements by Allan[26] and checked with momentum transfer cross sections obtained from the analysis of electron swarm parameters, see Sec. 4. The uncertainty on such an evaluation is ±5%.

At high energies, in the range of 1–4 keV, our recommended values are based on measurements by Ariyasinghe *et al.*[19] who used a linear transmission method with a retarding-field analyzer. As we show in Born–Bethe plot presented in Fig. 2, the data of Ariyasinghe are slightly lower than those of García and Manero.[20] As discussed for NH_3 by Zecca *et al.*,[27] their data are underestimates in the high-energy limit (due

TABLE 2. Summary of total cross section measurements used to obtain our recommended values. The overall uncertainty on the recommended TCS in the whole 0.001–5000 eV energy range is ±5%

Authors	Energy range, declared errors	Scattering cell length SC apertures	Methods
Ferch *et al.* (1985)[12]	0.085–12 eV, 1%–4.5% stat., syst. < 1%	271 mm, ϕ = 2.0 mm	Absolute, time of flight, weak magnetic focusing
Lohmann and Buckman (1986)[13]	0.1–20 eV, 3%–5% stat.	255 mm, ϕ = 2.0 mm	Absolute, time of flight, weak magnetic focusing
Jones (1985)[14]	1.3–50 eV, 3%–9% total	380 mm, ϕ = 2.0 mm	Absolute, time of flight
Szmytkowski (1991, from Zecca *et al.*[15])	0.4–100 eV, 3% stat, 4% syst.	30.5 mm, 0.35 × 0.7 mm	Absolute, linear transmission, cylindricalelectrostatic monochromator
Dababneh *et al.* (1988)[16]	1.5–500 eV, 5% + ang. resolution error	109 cm, 3° – 28° collection angle	Absolute, transmission, magnetic guiding, positron and electron scattering
Nishimura and Sakae (1990)[17]	5–500 eV, 13% syst., 1%–5% stat.	25 mm + 1 cm drift ϕ = 1.0 – 2.0 mm	Absolute, linear transmission, angular resolution extrapolated to zero
Kanik *et al.* (1992)[18]	4–300 eV, 2.1%–3.3%		Total absolute, linear transmission, electrostatic gun
Zecca *et al.* (1991)[15]	75–4000 eV, 2.5% sys., 3% stat.; –30% ang. res. at 4 keV	140 mm + 120 mm drift, 3 × 5 mm exit	Absolute, Ramsauer-like, high-energy experiment, double scattering cell, no retarding-field analyzer
Ariyasinghe *et al.* (2004)[19]	300–4000 eV, 4% total	245 mm, ϕ = 1.0 mm	Absolute, linear transmission, with retarding-field analyzer
García and Manero (1998)[20]	400–5000 eV, 2% stat., 3% syst.	70–127 mm, ϕ = 1.0 mm,	Absolute, linear transmission, with retarding-field analyzer
Barbarito *et al.* (1979)[21]	0.05–16 eV	40 mm, ϕ = 1.0 mm	Absolute, linear transmission, electrostatic gun
Sueoka and Mori (1986)[22]	1–400 eV	63.8 mm (71.7 mm effective) ϕ = 8.0 mm	Normalized, linear, magnetic guiding, positron and electron scattering
Floeder *et al.* (1985)[23]	5–400 eV, 5% stat., 3% syst.	515 mm, ϕ = 3.0 mm	Absolute, linear, weak magnetic focusing, positron and electron scattering

to the above mentioned lack of retarding-field analyzer) but those by García and Manero can be slightly (by few per cent) overestimates. To evaluate the quality of data in the high energy limit, in Fig. 2, we perform a Born–Bethe analysis by making the plot

$$\sigma(E) = A/E + B\log(E)/E \quad (2)$$

where energy is expressed in Rydbergs, Ry = 13.6 eV and the cross sections is expressed in atomic units $a_0^2 = 0.28 \times 10^{-16}$ cm^2. As seen from the figure, the TCS of Ariyasinghe *et al.*[19] can be fitted by a straight-line with $A = 52 \pm 17$ and $B = 232 \pm 9$.

Three sets of data were excluded from the analysis. Barbarito *et al.*[21] obtained cross sections, which agree in shape with other sets, but are significantly lower. This discrepancy is probably due to very short (about 1 min) gas on/off cycles. Similar discrepancies with other experiments are present in electron—NO and N_2O measurements by the same group.[28] Floeder *et al.*[23] used a weak focusing magnetic field in their apparatus designed for positron and electron scattering. Their data are on average lower by 5% than the recommended set. Sueoka and Mori[22,29,30] also used an apparatus designed essentially for positron-scattering experiments. Based on their early measurement on N_2, for all subsequent results, they adopted an "effective" length for their scattering cell (72 mm), which differs by about 10% from the geometrical length (64 mm). This could have led to two types of systematic-calibration: underestimation of the absolute cross sections by a constant relative value and an energy shift, changing with energy, due to the time-of-flight method employed. On average, Sueoka and Mori's data are about 10%–15% lower than other measurements. Similar discrepancies are seen in other targets, such as NH_3 and H_2O.[22,29,30] The early measurements of Ramsauer and Kollath[31] at 0.1–1.2 eV agree very well with those by Ferch *et al.*[12] and Lohmann and Buckman.[13] However, the experimental results obtained using a similar method (a perpendicular magnetic field) by Brüche[32,33] and Brode[34] above 2 eV agree rather poorly with modern measurements.

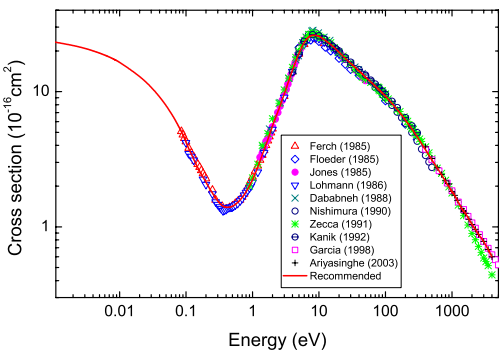

FIG. 1. Comparison of experimental and recommended total cross sections in methane. See text for details.

3. Elastic Scattering Cross Section

There have been many experimental investigations of elastic electron scattering from methane and the most relevant results

TABLE 3. Recommended TCS for electron scattering from methane in the units of 10^{-16} cm^2. Data in the energy ranges 0–0.1, 0.1–1000, and 1000–4000 eV are obtained using complementary procedures, see text for details. The overall uncertainty on the recommended TCS is ±5% over the whole energy range

Electron energy (eV)	TCS	Electron energy (eV)	TCS
0.001	23.38	10	25.7
0.002	21.97	12	24.3
0.005	19.29	15	22.3
0.007	18.03	17	21.2
0.01	16.51	20	19.6
0.02	13.07	25	17.6
0.03	10.82	30	16.2
0.04	9.18	35	15.1
0.05	7.91	40	14.2
0.06	6.89	45	13.5
0.07	6.06	50	12.8
0.08	5.37	60	11.8
0.09	4.79	70	11.0
0.1	4.25	80	10.3
0.12	3.45	90	9.75
0.15	2.72	100	9.24
0.17	2.46	120	8.38
0.2	2.13	150	7.37
0.25	1.77	170	6.83
0.3	1.55	200	6.16
0.35	1.42	250	5.30
0.4	1.39	300	4.66
0.45	1.40	350	4.10
0.5	1.41	400	3.71
0.6	1.51	450	3.38
0.7	1.64	500	3.11
0.8	1.81	600	2.74
0.9	2.01	700	2.42
1.0	2.23	800	2.17
1.2	2.76	900	1.97
1.5	3.73	1000	1.82
1.7	4.42	1100	1.71
2.0	5.64	1200	1.57
2.5	7.43	1400	1.36
3.0	9.60	1500	1.31
3.5	12.0	1600	1.26
4.0	14.5	1800	1.14
4.5	16.9	2000	1.04
5.0	19.3	2225	0.96
6.0	23.4	2500	0.88
7.0	25.6	3000	0.78
8.0	26.2	3500	0.68
9.0	26.1	4000	0.60

considered in this evaluation are listed in Table 4 with their experimental range and a few remarks. Even though there are many more reports on elastic scattering, the following data sets were excluded from the further considerations:

- relative measurements,
- data with no uncertainties.

The eight data sets, given in the Table 4, are used to derive the recommended elastic differential cross section (DCS) and integral cross section (ICS) after the following processes:

- remove data points which are too far off the general pattern,
- remove data points which have no other data points overlapped in the angular and energy region of interest,

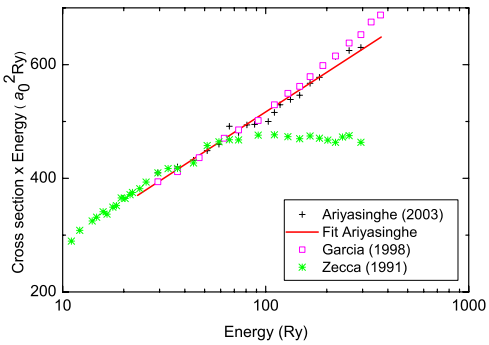

FIG. 2. Total electron scattering cross sections in methane in the high energy limit—Born–Bethe plot.

- average the remaining data to derive the recommended data sets,
- estimate the uncertainties of the recommended data.

We finally derived 13 sets of the recommended elastic electron scattering differential cross sections at different energies ranging from 1 eV to 500 eV.

Complete numerical data and 4 representative figures for elastic DCS's are presented in Table 5 and Fig. 3, respectively. The lines connecting the recommended data are given as guides. The recommended ICS's are presented in both graphic and tabulated form, respectively, in Fig. 4 and Table 6.

4. Momentum Transfer Cross Section

The momentum transfer cross section is defined by

$$\sigma_{MT} = 2\pi \int_0^{\pi} \frac{d\sigma}{d\theta} \sin\theta(1 - \cos\theta)d\theta. \quad (3)$$

Analysis of momentum transfer cross sections from beam experiments is based on the same criteria as the elastic cross sections: both momentum transfer and integral elastic cross sections are obtained by integrating differential cross sections. Therefore, similar confidence criteria apply to momentum transfer as to integral elastic cross sections. Additionally, momentum transfer cross sections can be obtained from analysis of swarm experiments, see Sec. 6. A comparison of beam and swarm-derived momentum transfer cross sections is given in Fig. 5. Momentum transfer cross sections (MTCS) are more sensitive to uncertainties at high scattering angles than the integral elastic cross sections, see Eq. (3). Therefore, experiments at high angles are important. Out of several data sources listed in Table 4, the measurements by Shyn and Cravens,[41] who used an electrostatic analyzer extending up to 168°, and Allan[35] and Cho *et al.*,[38] who used a magnetic-field angle-changer extending up to 180°, sample high angles. Two sets of data by Tanaka and collaborators[36,43] differ in the spectrometers used, the normalization procedures, and extrapolation formula for differential cross sections. The newer MTCS[36] are higher than the earlier ones by some 30% and give the highest cross sections about the maximum at Fig. 5. MTCS by Cho *et al.*[38] and Shyn and Cravens[41] are the lowest sets

TABLE 4. List of the publications considered in deriving the recommended elastic cross sections with energy and angular ranges used in the measurements

Authors	Energy range (eV)	Angular range (°)
Allan (2007)[35]	0.4–20	10–180
Boesten and Tanaka (1991)[36]	1.5–100	10–130
Bundschu *et al.* (1997)[37]	0.6–5.4	12–132
Cho *et al.* (2008)[38]	5–100	10–180
Iga *et al.* (2000)[39]	100–500	10–135
Sakae *et al.* (1989)[40]	75–700	5–135
Shyn and Cravens (1990)[41]	5–50	12–156
Sohn *et al.* (1986)[42]	0.2–5	15–138

at the cross section maximum. The measurements by Allan, recorded with 1° grid, fall in the middle of these extremes and agree well with the MTCS of Tanaka *et al.*,[43] Bundschu *et al.*[37] at lower and Castro *et al.*[44] at higher energies. In the very-low energy region, modeling of swarm parameters is very sensitive to the correct choice of MTCS. However, in methane, the Ramsauer–Townsend (R–T) minimum of the MTCS, at 0.3 eV, falls exactly at the maxima of the unresolved v_2 and v_4 vibrational modes, making swarm analysis difficult. In fact, several authors derived MTCS values ranging at the minimum from 0.25×10^{-16} cm^2 to 1.0×10^{-16} cm^2,[45–50] in order of rising values. Some other sets of swarm-derived cross sections for methane are available on the internet.[51]

Modified effective range theory is expected to match with the elastic and momentum transfer cross sections in the low energy range. However, due to the high value of the dipole polarizability, the applicability of this method in methane is limited to energies below 0.5 eV.[50] In a new approach,[25] this limit was raised to 1 eV, therefore enabling the analysis in the R–T minimum. MTCS derived in this way agree in the minimum region both with electron swarm parameters, as well as with recent beam measurements.[35] MTCS due to Sohn *et al.*[42] in the region of R–T minimum can be affected, as stated by the authors, by higher errors; the cross sections at 0.5 eV were determined in different runs.[52] The comparison of the *p*-wave phase shifts between 0.2 and 0.5 eV (see Fig. 2 of Sohn *et al.*[42]) suggests that the integral and MTCS of Sohn *et al.*[42] are overestimated in this energy range. Therefore, in Fig. 5, we show, together with the original values from Sohn *et al.*,[42] the values reduces somewhat arbitrarily by 0.5×10^{-16} cm^2 (see Fedus and Karwasz[25]). Our recommended MTCS, in the region of R–T minimum based on the model of Fedus and Karwasz, agree with the corrected MTCS of Sohn *et al.*[42] In the high energy range, the spread of experimental MTCS due to Cho *et al.*,[38] Sakae *et al.*,[40] and Iga *et al.*,[39] which is beam-derived and usually uses theory to extrapolate differential cross sections, is about ±10%, and the exceptions are the MTCS of Vušković and Trajmar.[53] At 100 eV, the data of Sakae *et al.*[40] are intermediate to those of Cho *et al.* and Iga *et al.*, see Fig. 5. Our recommended momentum transfer cross section shown in Table 7 is based on the following:

- from 0.001 eV to 1 eV on the modified effective range theory analysis of elastic differential, and of total cross section by Fedus and Karwasz;[25]
- from 1 eV to 12 eV on swarm-derived data by Kurachi and Nakamura,[45] which are in agreement with recent beam experiment by Allan[35] in 0°–180° angular range;
- from 15 eV to 50 eV on the recommended Landolt–Börnstein[54] data;
- from 75 eV to 300 eV on beam experiment by Sakae *et al.*[40]

We estimate the uncertainty bar on the recommended values in the whole energy region considered as ±10%.

5. Rotational Excitation Cross Section

The methane molecule does not have permanent dipole and quadrupole moments in the ground vibrational state. The lowest non-vanishing multipole moment is the octupole moment, which is about 3.0×10^{-34} esu cm^3 = 4.22 e a_0^3.[55] Therefore, in collisions where vibrational modes are not excited, when the initial rotational state is $J = 0$, the possible final rotational states should have $J \geq 3$.

It is almost impossible to resolve each rotational contribution in an energy loss peak of a beam measurement in experimental studies of rotational excitation due to present limitation on energy resolution. However, Ehrhardt and his group[52] devised a method of deconvolution of the elastic peak in the electron energy loss spectrum to obtain rotational cross section, see the review by Itikawa and Mason.[56] With the use of the adiabatic nuclear rotation approximation, they could express any rotational cross section as a linear combination of the cross section $q(0 \rightarrow J)$, which is the cross section for the transition from the ground to the Jth rotational states. To derive the rotational cross section of CH_4, Müller *et al.*[52] retained the cross sections $q(0 \rightarrow J)$ with $J = 0, 3, 4$ as the fitting parameters. Müller *et al.*[52] obtained only the DCS in the range of 15°–150°at 0.5 and 7.5 eV, and for 75°–150°at 5 and 10 eV. They give no integral cross section.

Theoretically, there are two classes of calculations: close-coupling method and variational calculation, see Itikawa and Mason[56] for details. Three papers[57–59] have been published based on close-coupling calculation for CH_4. Among them, Abusalbi *et al.*[57] reported the cross section only at one energy (10 eV). Gianturco *et al.*[58] and McNaughten *et al.*[59] used a similar method of calculation, but McNaughten *et al.*[59] adopted a more elaborate model of the interaction potential. Two groups[60,61] calculated rotational cross sections of CH_4

TABLE 5. Recommended elastic electron scattering cross sections from methane. DCS and δ indicate cross sections and uncertainties, respectively, in the units of 10^{-16} cm^2 sr^{-1}

Angle	1 eV		1.5 eV		2 eV		3 eV		5 eV		10 eV		20 eV	
(°)	DCS	δ	DCS	δ	DCS	δ	DCS	δ	DCS	δ	DCS	δ	DCS	δ
10											7.938	1.44	9.247	1.185
15					0.292	0.1	0.582	0.158	3.345	0.693	7.111	1.26	7.96	1.194
20			0.127	0.052	0.186	0.054	0.403	0.086	2.763	0.836	6.163	1	6.672	1.028
25			0.091	0.038	0.136	0.029	0.33	0.061	2.197	0.509	5.405	0.902	5.394	1.133
30	0.012	0.006	0.055	0.019	0.136	0.024	0.32	0.069	1.691	0.172	4.604	0.806	4.116	0.863
35	0.014	0.007	0.077	0.026	0.156	0.049	0.368	0.093	1.412	0.166	3.869	0.744	3.182	0.955
40	0.015	0.008	0.099	0.018	0.226	0.061	0.479	0.11	1.267	0.144	3.182	0.647	2.248	0.664
45	0.043	0.021	0.158	0.029	0.331	0.076	0.611	0.134	1.268	0.15	2.582	0.519	1.711	0.411
50	0.07	0.018	0.218	0.043	0.449	0.09	0.766	0.127	1.28	0.167	2.127	0.31	1.175	0.283
55	0.1	0.025	0.289	0.057	0.546	0.102	0.921	0.144	1.4	0.182			0.941	0.254
60	0.129	0.038	0.359	0.058	0.641	0.115	1.049	0.167	1.5	0.188	1.598	0.327	0.707	0.189
65	0.157	0.046	0.41	0.066	0.733	0.127	1.163	0.181	1.593	0.215			0.616	0.123
70	0.185	0.054	0.46	0.07	0.772	0.142	1.209	0.202	1.668	0.25	1.182	0.183	0.524	0.105
75	0.214	0.063	0.487	0.074	0.798	0.137	1.231	0.198	1.673	0.274	1.067	0.193	0.458	0.096
80	0.243	0.061	0.513	0.071	0.796	0.141	1.176	0.181	1.641	0.274	0.934	0.19	0.392	0.082
85	0.244	0.061	0.5	0.069	0.77	0.144	1.085	0.171	1.519	0.242	0.787	0.198	0.341	0.079
90	0.244	0.056	0.487	0.062	0.716	0.124	0.983	0.174	1.385	0.23	0.631	0.195	0.29	0.067
95	0.241	0.055	0.458	0.059	0.644	0.109	0.851	0.16	1.15	0.177	0.533	0.173	0.258	0.054
100	0.237	0.053	0.429	0.056	0.581	0.105	0.71	0.149	0.936	0.135	0.431	0.135	0.226	0.048
105	0.221	0.05	0.381	0.05	0.48	0.1	0.545	0.141	0.691	0.099	0.346	0.089	0.218	0.041
110	0.205	0.041	0.334	0.045	0.388	0.089	0.401	0.114	0.462	0.095	0.271	0.064	0.21	0.039
115	0.186	0.037	0.279	0.038	0.299	0.081	0.27	0.086	0.288	0.108	0.237	0.043	0.235	0.04
120	0.166	0.035	0.224	0.045	0.217	0.074	0.179	0.041	0.175	0.075	0.231	0.047	0.26	0.043
125	0.144	0.03	0.191	0.038	0.153	0.068	0.106	0.028	0.169	0.089			0.301	0.051
130	0.122	0.026	0.157	0.044	0.104	0.052	0.104	0.019	0.231	0.085			0.342	0.06
135													0.382	0.067
140													0.423	0.088

Angle	30 eV		50 eV		100 eV		200 eV		300 eV		500 eV	
(°)	DCS	δ	DCS	δ	DCS	δ	DCS	δ	DCS	δ	DCS	δ
10	10.053	1.283	9.46	1.6	8.215	3.608	5.633	0.822	3.969	0.642	2.969	0.482
15	8.082	1.142	6.727	0.854	4.928	1.038	2.472	0.369	1.506	0.31	0.985	0.144
20	6.112	0.864	3.994	0.507	1.985	0.519	0.918	0.169	0.626	0.128	0.462	0.066
25	4.593	0.969	2.787	0.692	1.103	0.186	0.486	0.079	0.357	0.071	0.261	0.038
30	3.075	0.649	1.58	0.392	0.468	0.12	0.315	0.049	0.234	0.04	0.157	0.023
35	2.258	0.518	1.102	0.265	0.334	0.062	0.223	0.035	0.149	0.025	0.099	0.016
40	1.442	0.331	0.625	0.15	0.211	0.069	0.147	0.022	0.105	0.017	0.065	0.01
45	1.074	0.198	0.46	0.077	0.162	0.059	0.104	0.016	0.074	0.012	0.043	0.006
50	0.706	0.13	0.296	0.05	0.113	0.05	0.076	0.012	0.057	0.009	0.031	0.005
55	0.557	0.099	0.244	0.051	0.083	0.034	0.06	0.009	0.044	0.007	0.022	0.004
60	0.408	0.073	0.192	0.04	0.055	0.029	0.05	0.008	0.037	0.005	0.018	0.003
65	0.349	0.066	0.153	0.041	0.044	0.02	0.043	0.007	0.03	0.005	0.014	0.002
70	0.289	0.056	0.114	0.031	0.035	0.016	0.037	0.005	0.024	0.004	0.011	0.002
75	0.246	0.064	0.094	0.021	0.03	0.014	0.034	0.005	0.021	0.003	0.009	0.002
80	0.204	0.053	0.074	0.016	0.026	0.014	0.032	0.005	0.017	0.003	0.008	0.002
85	0.173	0.05	0.063	0.013	0.027	0.014	0.029	0.004	0.015	0.002	0.007	0.001
90	0.142	0.041	0.051	0.011	0.028	0.015	0.027	0.004	0.013	0.002	0.006	0.001
95	0.135	0.027	0.049	0.01	0.03	0.015	0.024	0.004	0.012	0.002	0.005	0.001
100	0.128	0.025	0.046	0.009	0.032	0.015	0.022	0.004	0.011	0.002	0.005	0.001
105	0.129	0.025	0.054	0.011	0.035	0.016	0.021	0.004	0.011	0.002	0.004	0.001
110	0.13	0.026	0.063	0.013	0.038	0.015	0.02	0.004	0.01	0.002	0.004	0.001
115	0.15	0.029	0.074	0.016	0.04	0.017	0.019	0.003	0.01	0.002	0.004	0.001
120	0.169	0.033	0.086	0.018	0.041	0.018	0.018	0.003	0.01	0.002	0.004	0.001
125	0.192	0.036	0.097	0.02	0.044	0.019	0.019	0.003	0.009	0.002	0.003	0.001
130	0.214	0.04	0.107	0.023	0.045	0.01	0.019	0.003	0.009	0.002	0.003	0.001
135							0.021	0.003	0.009	0.001	0.003	0.001
140												

based on the Schwinger multichannel variational method. They used a very similar formulation for the calculation of the cross section, but Varella *et al.*[61] adopted a simpler model of interaction than Brescansin *et al.*[60] For instance, Varella *et al.* considered no polarization of the target molecule. More recently, the Brescansin group published a further paper;[62] they used a formulation slightly different from their previous one.[60] They reported only DCS at three energies.

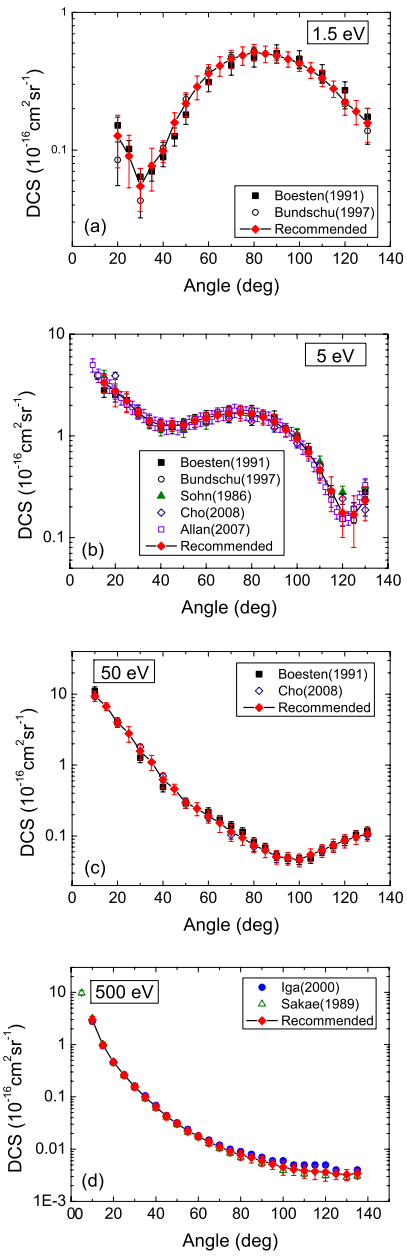

FIG. 3. Recommended elastic scattering cross sections with the selected sets of data from the publications at four representative energies.

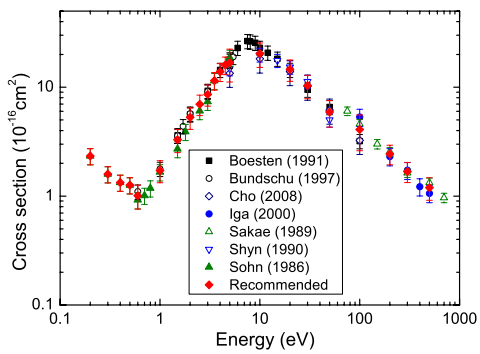

FIG. 4. Recommended elastic integral cross sections compared with the selected sets of data from the source publications.

TABLE 6. Recommended elastic ICS's for methane. The ICS and uncertainty, δ, are given in the units of 10^{-16} cm^2

Energy (eV)	ICS	δ
0.2	2.33	0.4
0.3	1.59	0.27
0.4	1.33	0.23
0.5	1.26	0.21
0.6	1.01	0.25
1.0	1.72	0.39
1.5	3.30	0.79
2.0	5.29	1.18
2.5	6.97	1.48
3.0	8.58	1.89
3.5	11.5	2.11
4.0	13.86	2.59
4.5	15.97	2.95
5.0	16.76	5.59
10	20.34	5.14
20	14.55	3.25
30	10.34	2.5
50	5.91	1.62
100	4.09	1.48
200	2.44	0.5
300	1.68	0.35
500	1.20	0.28

Recently Brigg *et al.*[63] have performed an R-matrix study of rotational excitation below 10 eV. Their results for the total cross section are in reasonable agreement with those of Brescansin *et al.*[60] and Abusalbi *et al.*[57] Figure 6 shows the comparison of rotational excitation cross sections from Refs. 57, 59, 60, and 63. Figures 7 and 8 show the DCS at 10 eV. The experimental values are available only from 75°to 150°. Figure 7 shows a large discrepancy between theory and experiment for the transition $J = 0 \rightarrow 3$. Figure 8 shows, however, that the cross sections of McNaughten *et al.* for $J = 0 \rightarrow 4$ agree well with the experimental one, while the two sets theoretical cross sections disagree with each other. Although not shown here, the calculation of Machado *et al.*[62] gives similar values to the results of McNaughten *et al.*[59] in this case.

Concluding, our recommended rotational excitation cross section shown in Tables 8 and 9 is based on the data by Brigg *et al.*,[63] because they are obtained in high-accuracy

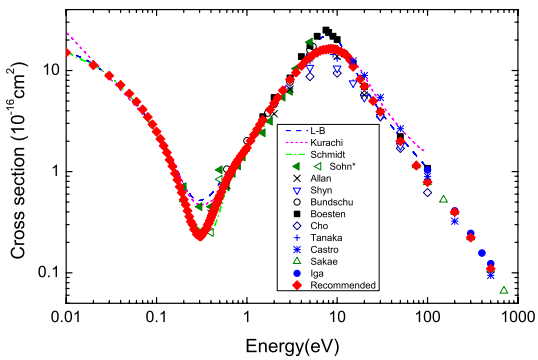

FIG. 5. Comparison of beam-derived, swarm-derived and recommended (present and Landolt–Börnstein[54]) momentum transfer cross sections for methane. Open triangles in the region of Ramsauer–Townsend minimum, labeled Sohn *et al.*,[42] are obtained after correcting their p-wave contribution to the measured differential cross sections, see text.

TABLE 7. Recommended MTCS for electron scattering in methane. Data in the energy ranges 0–0.1, 0.1–1000, and 1000–4000 eV have been obtained with complementary procedures, see text for details. MTCS are given in the units of 10^{-16} cm^2 and the uncertainty is ±10%

Electron energy (eV)	MTCS	Electron energy (eV)	MTCS	Electron energy (eV)	MTCS
0.001	22.8	0.30	0.23	1.2	2.32
0.002	21.2	0.31	0.23	1.3	2.62
0.003	19.9	0.32	0.24	1.4	2.93
0.004	19.0	0.33	0.25	1.5	3.24
0.005	18.1	0.34	0.26	1.8	4.11
0.006	17.4	0.35	0.27	2.0	4.77
0.007	16.7	0.36	0.28	2.2	5.41
0.008	16.1	0.37	0.30	2.5	6.34
0.009	15.5	0.38	0.31	3.0	8.12
0.01	15.0	0.39	0.33	3.5	9.54
0.02	11.3	0.40	0.35	4.0	11.1
0.03	8.89	0.41	0.37	4.5	12.5
0.04	7.20	0.42	0.39	5.0	13.5
0.05	5.92	0.43	0.41	5.5	14.5
0.06	4.92	0.44	0.43	6.0	15.1
0.07	4.12	0.45	0.46	6.5	15.7
0.08	3.47	0.46	0.48	7.0	16.0
0.09	2.93	0.47	0.50	7.5	16.1
0.10	2.49	0.48	0.53	8.0	16.3
0.11	2.11	0.49	0.55	8.5	16.4
0.12	1.80	0.50	0.58	9.0	16.3
0.13	1.54	0.52	0.63	9.5	16.2
0.14	1.31	0.55	0.70	10	16.0
0.15	1.13	0.57	0.75	11	15.3
0.16	0.96	0.60	0.83	12	14.6
0.17	0.83	0.62	0.88	13	13.5
0.18	0.71	0.65	0.95	14	12.1
0.19	0.62	0.67	1.00	15	11.0
0.20	0.53	0.70	1.07	18	8.20
0.21	0.47	0.72	1.12	20	6.93
0.22	0.41	0.75	1.18	25	4.99
0.23	0.36	0.77	1.24	30	3.92
0.24	0.32	0.80	1.33	50	2.00
0.25	0.30	0.85	1.45	75	1.15
0.26	0.27	0.90	1.56	100	0.79
0.27	0.26	0.95	1.67	200	0.40
0.28	0.24	1.00	1.80	300	0.22
0.29	0.24	1.10	2.07	500	0.11

calculations and agree reasonably well with the previous calculations. The agreement with the experimental and other theoretical results suggests that the uncertainty of the calculated results is probably about 10%. Notice that the rotational excitation was not included in the analysis of swarm experiments discussed in Sec. 6 mainly because at energies below a few eV, and the rotational cross sections are too small to have an effect on measured swarm parameters.

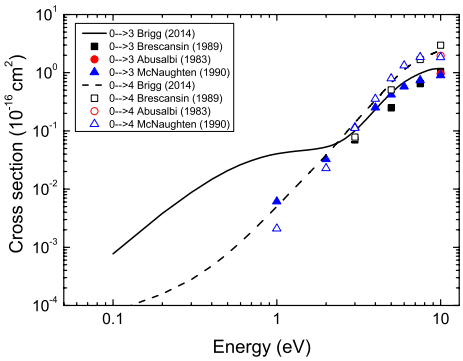

FIG. 6. Recommended cross sections for rotational excitation $J = 0 \rightarrow 3$ (solid line) and $J = 0 \rightarrow 4$ (dashed line) from Brigg *et al.* (2014).[63] For comparison, previous calculations by Abusalbi *et al.*,[57] McNaughten *et al.*[59] and Brescansin *et al.*[60] are shown as symbols.

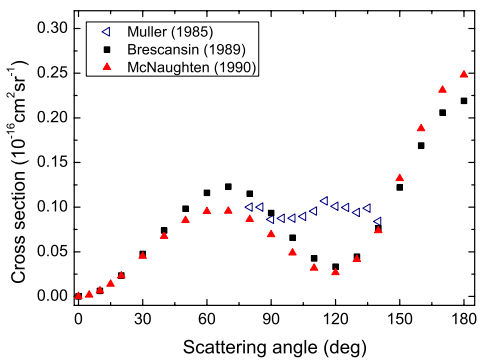

FIG. 7. Differential cross sections for the rotational transition $J = 0 \rightarrow 3$ for CH_4 at 10 eV. Comparison of the experimental data of Müller *et al.*[52] and the theoretical results of McNaughten *et al.*,[59] and Brescansin *et al.*[60]

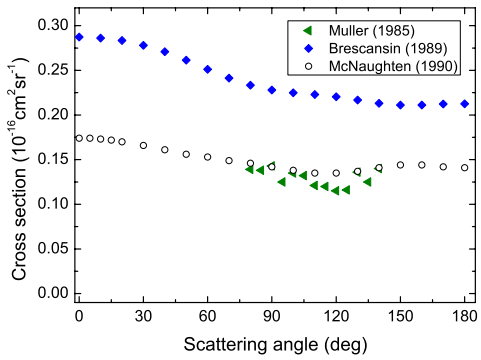

FIG. 8. Same as Fig. 7, but for the transition, $J = 0 \rightarrow 4$.

6. Vibrational Excitation Cross Sections

There are insufficient experimental data on vibrational excitation cross sections to cover the energy interval from 0.1 eV to 20 eV. Three different experiments by Tanaka *et al.*,[64] Shyn *et al.*,[65] and Bundschu *et al.*[37] gave results that disagree with each other by between 10% and 100%. On the other hand, there have been considerable theoretical efforts to calculate the cross sections for vibrational excitation. Čurik *et al.*[66] calculated the cross sections over 1–20 eV energy range taking into account non-adiabatic couplings between electronic and vibrational motion from first principles. Also, exact static-exchange contributions and correlation–polarization forces are included; this level of accuracy was not employed in the previous theoretical studies. Althorpe *et al.*,[67] presented integral cross sections for vibrational excitation cross sections between 0.05 and 12 eV, which were calculated from the off-shell scattering amplitudes, using a single-center expansion approach. Non-adiabatic effects were taken into account in this treatment. These two calculations disagree to a certain degree for excitation of the ν_1 and ν_4 modes: the cross sections of Althorpe *et al.* are smaller than those from Čurik *et al.* by about factor of 2.4 for the ν_1 mode and by a factor of 0.9 for the ν_4 mode. The results of Čurik *et al.*[66] are evaluated as being more precise than those of Althorpe *et al.*[67] for energies above 4 eV, but they do not extend below 1 eV. In this situation, the data of Althorpe *et al.* for the ν_1 and ν_4 mode are scaled in order to have smooth theoretical cross sections.

There is another data source for vibrational excitation cross sections from electron swarm studies.[45,68] Accuracy expected for measured electron swarm parameters is generally high. Typical uncertainty is ±1%–2% for the electron drift velocity, ±3%–5% for the ratio of the transverse diffusion coefficient to the electron mobility D_T/μ, ±5%–6% for the density normalized longitudinal diffusion coefficient ND_L, and ±2%–5% for the density normalized ionization and attachment coefficients, α/N and η/N. Analytical procedures for calculating these swarm parameters from electron collision cross section data, such as Boltzmann equation analysis and Monte Carlo calculation, are well established. In electron swarm study, a set of electron collision cross sections is derived, in a trial-and-error manner, in order that the set gives swarm parameters consistent with the measurements. When a small amount of a molecular gas is added to pure argon gas, the electron drift velocity in the mixture frequently shows a remarkable E/N dependence: Mixing one percent of molecule into argon enhances electron the drift velocity of argon by almost an order of magnitude. This is caused by the vibrational excitation collisions of electrons, and the effect is amplified by the Ramsauer–Townsend minimum of the argon momentum transfer cross section which is sufficiently well known. The momentum transfer cross section

TABLE 8. Recommended cross sections for rotational excitation $J = 0 \rightarrow 3$ from Brigg *et al.*[63] Cross section are given in the units of 10^{-16} cm^2 and the uncertainty is ±10%

Electron energy (eV)	Cross section	Electron energy (eV)	Cross section
0.1	0.000 77	5.3	0.523
0.2	0.003 82	5.4	0.548
0.3	0.008 77	5.5	0.572
0.4	0.014 7	5.6	0.596
0.5	0.020 7	5.7	0.620
0.6	0.026 2	5.8	0.643
0.7	0.031 0	5.9	0.666
0.8	0.034 9	6	0.688
0.9	0.038 0	6.1	0.710
1	0.040 3	6.2	0.732
1.1	0.042 2	6.3	0.752
1.2	0.043 6	6.4	0.773
1.3	0.044 8	6.5	0.793
1.4	0.045 8	6.6	0.812
1.5	0.046 7	6.7	0.831
1.6	0.047 6	6.8	0.850
1.7	0.048 6	6.9	0.868
1.8	0.049 8	7	0.886
1.9	0.051 2	7.1	0.903
2	0.052 9	7.2	0.920
2.1	0.055 0	7.3	0.937
2.2	0.057 5	7.4	0.954
2.3	0.060 5	7.5	0.970
2.4	0.064 0	7.6	0.986
2.5	0.068 2	7.7	1.002
2.6	0.073 1	7.8	1.017
2.7	0.078 9	7.9	1.032
2.8	0.085 3	8	1.047
2.9	0.092 6	8.1	1.061
3	0.101	8.2	1.074
3.1	0.110	8.3	1.088
3.2	0.120	8.4	1.098
3.3	0.131	8.5	1.109
3.4	0.143	8.6	1.120
3.5	0.156	8.7	1.129
3.6	0.170	8.8	1.138
3.7	0.184	8.9	1.146
3.8	0.200	9	1.152
3.9	0.217	9.1	1.158
4	0.234	9.2	1.163
4.1	0.252	9.3	1.167
4.2	0.272	9.4	1.171
4.3	0.291	9.5	1.174
4.4	0.312	9.6	1.176
4.5	0.334	9.7	1.177
4.6	0.356	9.8	1.178
4.7	0.379	9.9	1.179
4.8	0.401	10	1.180
4.9	0.426	10.1	1.180
5	0.450	10.2	1.181
5.1	0.474	10.3	1.181
5.2	0.499	10.4	1.182

TABLE 9. Recommended cross sections for rotational excitation $J = 0 \rightarrow 4$ from Brigg *et al.*[63] Cross sections are given in the units of 10^{-16} cm^2 and the uncertainty is ±10%

Electron energy (eV)	Cross section	Electron energy (eV)	Cross section
0.1	0.000 08	5.3	0.802
0.2	0.000 16	5.4	0.849
0.3	0.000 28	5.5	0.895
0.4	0.000 47	5.6	0.942
0.5	0.000 78	5.7	0.989
0.6	0.001 22	5.8	1.036
0.7	0.001 84	5.9	1.083
0.8	0.002 66	6	1.129
0.9	0.003 72	6.1	1.174
1	0.005 04	6.2	1.219
1.1	0.006 64	6.3	1.262
1.2	0.008 55	6.4	1.304
1.3	0.010 78	6.5	1.344
1.4	0.013 4	6.6	1.384
1.5	0.016 3	6.7	1.421
1.6	0.019 7	6.8	1.459
1.7	0.023 6	6.9	1.494
1.8	0.028 0	7	1.529
1.9	0.032 9	7.1	1.563
2	0.038 5	7.2	1.596
2.1	0.044 7	7.3	1.629
2.2	0.051 7	7.4	1.661
2.3	0.059 5	7.5	1.693
2.4	0.068 1	7.6	1.725
2.5	0.077 6	7.7	1.756
2.6	0.087 9	7.8	1.788
2.7	0.099 2	7.9	1.819
2.8	0.111 5	8	1.851
2.9	0.124 7	8.1	1.882
3	0.138 8	8.2	1.914
3.1	0.153 9	8.3	1.945
3.2	0.170 0	8.4	1.977
3.3	0.187 1	8.5	2.008
3.4	0.205	8.6	2.039
3.5	0.224	8.7	2.069
3.6	0.244	8.8	2.098
3.7	0.266	8.9	2.127
3.8	0.288	9	2.154
3.9	0.313	9.1	2.181
4	0.337	9.2	2.205
4.1	0.363	9.3	2.228
4.2	0.391	9.4	2.250
4.3	0.420	9.5	2.269
4.4	0.451	9.6	2.286
4.5	0.484	9.7	2.300
4.6	0.518	9.8	2.313
4.7	0.554	9.9	2.323
4.8	0.592	10	2.331
4.9	0.631	10.1	2.337
5	0.672	10.2	2.342
5.1	0.714	10.3	2.348
5.2	0.758	10.4	2.358

of the molecule, on the other hand, has little effect on swarm parameters in the mixture because of the minor concentration of the molecule. The swarm parameters measured in a dilute molecular gas–argon gas mixture, therefore, can be a very good guide in deriving vibrational cross sections for the molecule. The swarm parameters measured in a pure molecular gas in low and medium E/N ranges depend on both the momentum

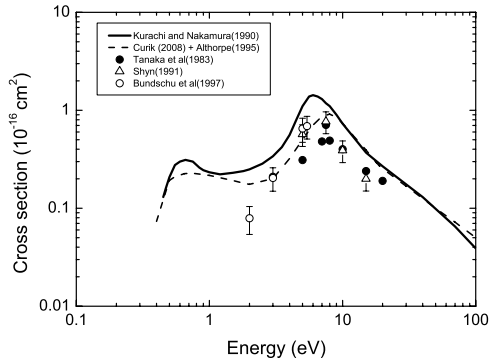

FIG. 9. Comparison of vibrational excitation cross sections for the ν_1 and ν_3 normal modes. Solid line, swarm derived; short broken line, theoretical (combination of Althorpe *et al.*[67] below 4 eV is multiplied by a factor of 2.4 and by Čurik *et al.*[66] above 4 eV); solid circle, Tanaka *et al.*;[64] open triangle, Shyn;[65] open circle, Bundschu *et al.*[37]

transfer and vibrational cross sections. Hence, alternate uses of swarm parameters measured in the mixtures and in the pure molecular gas can lead the momentum transfer and vibrational excitation cross sections of the molecule to their converged values. After the measurements of electron swarm parameters in pure methane[69] and in the 1.03% and 5.13% methane–argon mixtures,[70] Kurachi and Nakamura[45] derived a set of cross sections for the methane molecule by using the electron swarm study. Their vibrational cross sections are compared with those obtained through theoretical calculations, and also with those measured by beam experiments, in Figs. 9 and 10.

The swarm-derived vibrational cross sections are distinguishingly sharper at threshold peaks and higher at shape resonance peaks. The swarm parameters calculated by using these two sets of the vibrational excitation cross sections and the multi-term Boltzmann equation analysis,[71] which assumes isotropic scattering, are compared with the experimental results in the mixtures and also in pure methane in Figs. 11–14. The higher resonance peak of the swarm-derived cross sections is crucial for giving drift velocity and ND_L consistent with the experimental swarm parameters in pure methane[46,47,69,72,73] as well as in the methane–argon mixtures[70,74] over intermediate

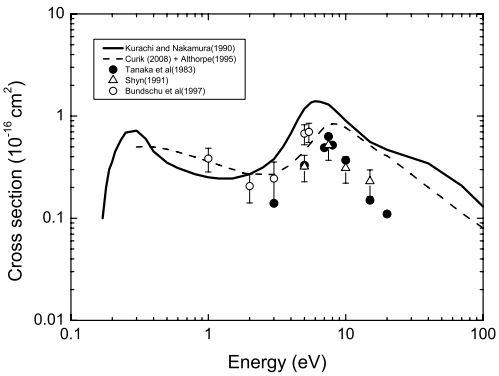

FIG. 10. Comparison of vibrational excitation cross sections for the ν_2 and ν_4 normal modes. Solid line, swarm derived; short broken line, theoretical (combination of Althorpe *et al.*[67] below 4 eV is multiplied by a factor of 0.8 and by Čurik *et al.*[66] above 4 eV); solid circle, Tanaka *et al.*;[64] open triangle, Shyn;[65] open circle, Bundschu *et al.*[37]

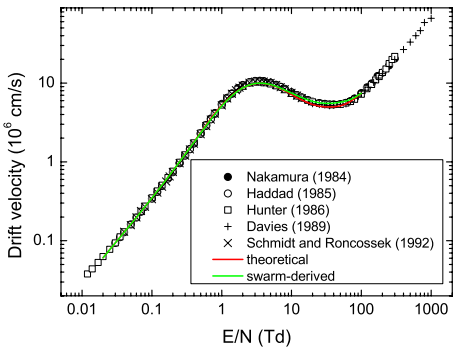

FIG. 11. Comparison of experimental and calculated electron drift velocities in pure methane. Plots show the experimental results, and the solid lines show the results of the multi-term Boltzmann equation analysis using the theoretical and swarm-derived vibrational excitation cross sections.

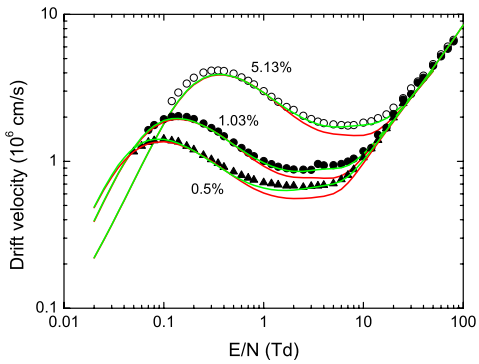

FIG. 13. Electron drift velocity in CH_4–Ar mixtures. Solid triangles, de Urquijo *et al.*;[74] solid and open circles, Obata *et al.*;[70] red lines, theoretical data and green lines, swarm-derived data.

and higher E/N as seen in these figures. We, therefore, recommend the swarm-derived cross sections for electron collision vibrational excitations of the methane molecule, which are given in Tables 10 and 11. The uncertainties in vibrational excitation cross section are about 15% at its peak and higher elsewhere.

7. Ionization Cross Section

Cross sections for electron-impact ionization of methane have been measured since the 1920s.[75] The more recent, 1960s, measurements of Rapp and Englander-Golden[76] extending up to 1000 eV are still in use. Rapp and Englander-Golden normalized their CH_4 results to their own absolute measurements in H_2. Partial cross sections by Adamczyk *et al.*[77] up to 1000 eV and Chatham *et al.*[78] up to 100 eV are lower than newer data, with particularly big differences for the lightest ions; as discussed below, this is due to an incomplete collection of energetic fragment ions in those early experiments. Djurić *et al.*[79] measured total ionization cross section up to 200 eV—their cross sections practically coincide with those of Rapp and Englander-Golden.[76] Nishimura and Tawara[80] measured absolute total ionization cross sections with an 8% systematic uncertainty. Their maximum cross section (3.98×10^{-16} cm^2) is in a very good agreement with more recent data by Straub *et al.*[81] Tarnovsky *et al.*[82] reported measurements of CD_4^+, CD_3^+, CD_2^+, and CD^+ ions from CD_4 using electrostatic hemispherical analyzer and normalizing data to their own measurements in Ar and Kr. Their data agree well with recent partial ionization cross sections of CH_4. Absolute measurements of the total ionization in CH_4 up to 200 eV by Vallance *et al.*[83] gave a maximum of the cross section of 4.2×10^{-16} cm^2, i.e., slightly higher than the value of Nishimura and Tawara, but at higher energies, the cross sections of Vallance *et al.* decrease too rapidly with energy. Tian and Vidal[84,85] used a time-of-flight spectrometer and normalized their partial cross sections to the Ar^+ cross section of Straub *et al.*[81] Gluch *et al.*[86] measured partial cross sections using a double-focusing mass spectrometer and normalized at 100 eV to the total cross section by Rapp and Englander-Golden; in Fig. 15 we show their data re-normalized by a factor of πa_0^2, i.e., to the original data of Rapp and Englander-Golden.[76] Partial cross sections were measured in an absolute manner by Straub *et al.*[87] with a time-of-flight and position-sensitive detector; the data were put on absolute scale by pressure measurements at 200 eV. Declared uncertainties are from 3.5% for total cross sections, CH_4^+ and CH_3^+ ions and somewhat higher for light ions, up to 7% for C^+. Recommended cross sections by Lindsay and Mangan[88] from Landolt–Börnstein collection are based on Straub *et al.*[87] but are lower by about 10% for all ions at 100 eV and by 1%–2% at 1000 eV. After a detailed analysis of the different data, supported by additional numerical and semi-empirical comparisons, we adopt the database of Lindsay and Mangan

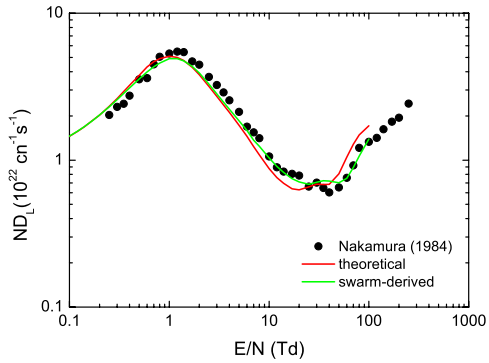

FIG. 12. The gas density normalized longitudinal diffusion coefficient ND_L in pure methane.

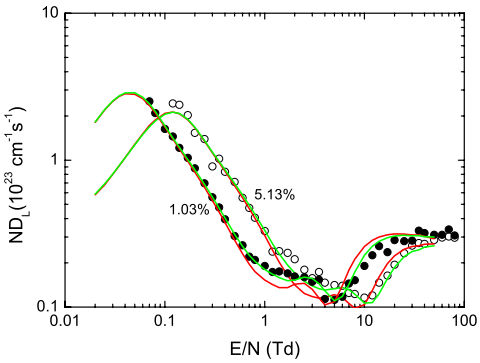

FIG. 14. Density-normalized longitudinal diffusion coefficient in CH_4-Ar mixtures. Symbols are the same as in Fig. 13.

TABLE 10. Recommended cross sections for vibrational excitation of the ν_1 and ν_3 normal modes. Cross sections are given in the units of 10^{-16} cm^2

Electron energy (eV)	Cross section	Electron energy (eV)	Cross section
0.362	0.000	3.5	0.420
0.45	0.130	4.0	0.560
0.47	0.160	4.5	0.800
0.50	0.208	5.0	1.100
0.55	0.276	5.6	1.380
0.60	0.299	6.0	1.430
0.66	0.312	6.5	1.380
0.75	0.299	7.0	1.300
0.84	0.260	7.5	1.180
0.90	0.245	8.0	1.100
1.0	0.233	9.0	0.900
1.2	0.222	10	0.730
1.5	0.230	15	0.364
1.8	0.240	20	0.286
2.0	0.250	40	0.169
2.5	0.285	70	0.065
3.0	0.340	100	0.039

also as our present recommended data, see Table 12 and Fig. 16. A rough evaluation of the uncertainties is ±5% for total ionization cross section and ± 10% for partial cross sections. Total ionization cross sections from selected experiments are compared in Fig. 15 and partial cross sections for CH_4^+ and CH_3^+ ions in Fig. 17.

7.1. Numerical interpolations

Several semi-empirical analyses were performed in the past on CH_4 ionization cross sections. Dose *et al.*[91] used simple formulas,

$$\sigma = c\frac{(x-1)^{\epsilon}\ln(x)}{a+(x-1)^{\epsilon}x} \tag{4}$$

TABLE 11. Recommended cross sections for vibrational excitation of the ν_2 and ν_4 normal modes. Cross sections are given in the units of 10^{-16} cm^2

Electron energy (eV)	Cross section	Electron energy (eV)	Cross section
0.162	0.000	3.0	0.380
0.17	0.100	3.5	0.500
0.18	0.200	4.0	0.680
0.19	0.300	4.5	0.930
0.20	0.360	5.0	1.180
0.21	0.450	5.6	1.360
0.23	0.580	6.0	1.400
0.25	0.690	6.5	1.380
0.30	0.720	7.0	1.340
0.35	0.600	7.5	1.300
0.4	0.450	8.0	1.200
0.5	0.350	9.0	1.040
0.6	0.310	10	0.900
0.8	0.270	15	0.560
1.0	0.252	20	0.468
1.2	0.245	40	0.345
1.5	0.245	70	0.208
2.0	0.270	100	0.130
2.5	0.315		

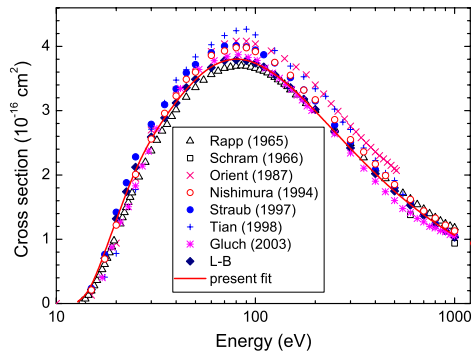

FIG. 15. Comparison of experimental gross total ionization cross section (total charge yield) for electron scattering from methane. The cross sections by Gluch *et al.*[86] are re-normalized by a factor of πa_0^2. The cross sections of Vallance *et al.*,[83] not shown for clarity, coincide near the maximum with those of Tian and Vidal[85] but above 100 eV fall quickly with energy. Cross sections of Adamczyk *et al.*,[77] Chatham *et al.*,[78] Djurić *et al.*[79] are not shown for clarity either. Present fit was made using formula Eq. (9).

and

$$\sigma = c\frac{(x-1)^{\epsilon}}{a+(x-1)^{\epsilon}x}, \tag{5}$$

where $x = E/I_i$, with E being collision energy and I_i being the ionization threshold for appearance of a given ion i. These two formulas have a straightforward physical interpretation; namely, Eq. (4) represents optically allowed processes. For their analysis, Dose *et al.*[91] used rather old data[77,78] so their parameters fit our recommended data rather poorly. We have re-tested their formulas for the recommended data, and the results are given in Table 13. Generally, the fits are acceptable, with differences within ±10% in the energy range of 50–1000 eV. Some larger differences are observed in the near-to-threshold region, where intrinsically the formulas (4) and (5) are not applicable. For C^+ and H^+, ions the formula (5) for forbidden transitions was used. For CH^+ it was necessary to slightly modify formula (4) to give

$$\sigma = c\frac{(x-1)^{\epsilon}\ln(x)}{a+(x-1)^{\epsilon}x^{1.18}}. \tag{6}$$

As seen from the Table 13, exponents ϵ in the fits are low (0.15–0.2) for the dominant ions (CH_4^+ and CH_3^+) and are

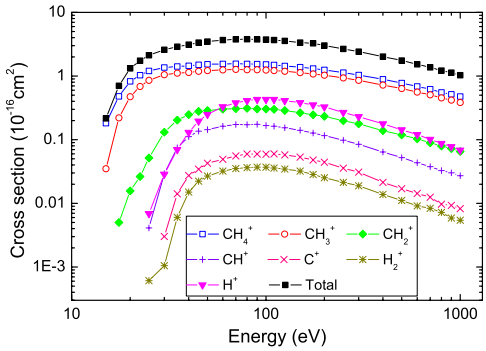

FIG. 16. Recommended partial and total cross sections for electron-scattering ionization in methane. These data correspond to those published in the Landolt–Börnstein database.[88]

TABLE 12. Recommended data (in units of 10^{-16} cm^2) for electron-scattering ionization of methane. Source: Lindsay and Mangan[88] and Landolt–Börnstein database

Electron energy (eV)	CH_4^+	CH_3^+	CH_2^+	CH^+	C^+	H_2^+	H^+	Total
15	0.182	0.035						0.216
17	0.479	0.220	0.005 0					0.703
20	0.825	0.474	0.015 7					1.32
22.5	1.03	0.685	0.026 4					1.74
25	1.20	0.857	0.051 8	0.004 1		0.000 61	0.006 9	2.12
30	1.36	1.05	0.131	0.0292	0.003 01	0.001 05	0.028 7	2.59
35	1.41	1.11	0.203	0.074 6	0.014 1	0.006 02	0.070	2.89
40	1.45	1.14	0.248	0.112	0.027 4	0.015 0	0.130	3.12
45	1.50	1.19	0.279	0.136	0.034 4	0.022 3	0.196	3.36
50	1.53	1.22	0.288	0.144	0.042 7	0.026 8	0.249	3.49
60	1.55	1.25	0.302	0.163	0.049 2	0.032 1	0.329	3.67
70	1.56	1.27	0.307	0.173	0.055 5	0.035 2	0.380	3.78
80	1.55	1.26	0.311	0.172	0.059 7	0.036 4	0.410	3.79
90	1.54	1.26	0.304	0.174	0.059 4	0.037 1	0.428	3.78
100	1.52	1.24	0.304	0.167	0.059 2	0.036 9	0.430	3.74
110	1.49	1.22	0.300	0.163	0.059 8	0.035 9	0.429	3.68
125	1.44	1.19	0.287	0.154	0.057 8	0.034 5	0.412	3.56
150	1.38	1.13	0.266	0.140	0.053 2	0.032 2	0.381	3.36
175	1.31	1.08	0.246	0.127	0.048 1	0.028 4	0.353	3.28
200	1.25	1.03	0.233	0.116	0.044 4	0.025 3	0.328	3.02
250	1.13	0.934	0.199	0.0981	0.035 6	0.021 4	0.268	2.67
300	1.04	0.855	0.177	0.0844	0.031 0	0.018 9	0.230	2.42
400	0.891	0.719	0.139	0.0643	0.021 3	0.013 8	0.177	2.02
500	0.778	0.638	0.119	0.0524	0.017 0	0.011 1	0.143	1.75
600	0.686	0.560	0.103	0.0435	0.014 3	0.009 11	0.120	1.53
700	0.623	0.507	0.0892	0.0378	0.012 5	0.008 34	0.101	1.37
800	0.552	0.454	0.0798	0.0327	0.009 72	0.007 21	0.0871	1.22
900	0.516	0.420	0.0726	0.0302	0.009 26	0.005 88	0.0774	1.13
1000	0.476	0.385	0.0654	0.0272	0.008 27	0.005 42	0.0688	1.03

around or higher than one for production of CH_2^+, CH^+, C^+, H_2^+, and H^+ ions. Shirai *et al.*[10] used the following formula with four fitting parameters a_1–a_4 for the total ionization cross section:

$$\sigma = a_1 \left[\ln(x + a_2)\right] / \left[\frac{E^2}{x}(1 + a_3/y)^{a_4}\right], \tag{7}$$

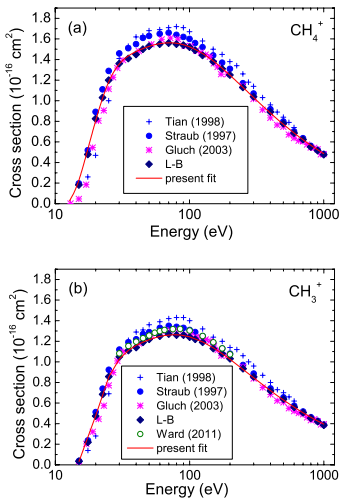

FIG. 17. Comparison of experimental partial ionization cross section for electron scattering from methane. The cross sections by Gluch *et al.*[86] are re-normalized by a factor of πa_0^2. The relative cross sections of Ward *et al.*[89] are normalized to CH_4^+ cross sections (present recommended data). The data of Adamczyk *et al.*,[77] Chatham *et al.*,[78] and Orient and Srivastava[90] are not shown for clarity. Present fit with formula Eq. (9), see Table 14.

and for partial ionization cross sections, the following expression with six adjustable parameters a_1–a_6:

$$\sigma = a_1 \left(\frac{y}{R}\right)^{a_2} \left[1 + \left(\frac{y}{a_3}\right)^{a_2+a_4} + \left(\frac{y}{a_5}\right)^{a_2+a_6}\right], \tag{8}$$

where $y = E - I_j$ is expressed in keV, $Ry = 0.013\,65$ keV is the Rydberg constant, and cross sections are expressed in 10^{-16} cm^2. The input cross sections were those of Nishimura and Tawara[80] and Straub *et al.*[81] The parameters given by Shirai *et al.* generally fit both our recommended total and partial cross sections well, apart from the threshold regions. Using the recommended data from Table 12, we obtained a new set of parameters that are given in Table 14. Generally, our fits using Eqs. (7) and (8) reproduce the total and partial ionization cross sections above 30 eV within ±5%. Janev and Reiter[11] used a six-parameter expression,

TABLE 13. Fits to the recommended partial ionization cross sections (Table 12) using the formulas from Dose *et al.*,[91] Eqs. (4) and (6). Coefficients c are in units of 10^{-16} cm^2

Ion	Formula	c	a	ϵ
CH_4^+	(4)	8.5	4.5	0.15
CH_3^+	(4)	6.2	3.4	0.2
CH_2^+	(5)	1.16	4.2	1
CH^+	(6)	0.6	0.67	1.7
C^+	(5)	0.35	8.4	1.2
H^+	(5)	3.9	22	1.2

TABLE 14. Fits to our recommended partial ionization cross sections (Table 12) using formulas from Shirai *et al.*:[10] Eqs. (7) and (8). Coefficients a_1 are in 10^{-16} cm^2 and the remaining coefficients are dimensionless

Process threshold (eV)	a_1	a_2	a_3	a_4	a_5	a_6	
Total	0.002 5	1.1759	0.065 4	1.1223	–	–	Present
12.63	0.003 539	0.036	0.037 3	0.906	–	–	Shirai
CH_4^+	9.660 2	2.3211	0.005 6	−0.2078	0.0187	0.9103	Present
12.63	4.886	1.627	0.007 42	−0.045	0.033	1.04	Shirai
CH_3^+	7.132 3	2.2621	0.005 6	−0.2343	0.0192	0.9075	Present
12.63	2.35	1.435	0.011 3	0.074	0.055	1.2	Shirai
CH_2^+	0.206 4	3.2928	0.015	−0.3132	0.0287	1.0065	Present
16.2	0.121	1.868	0.034 4	0.3	0.0552	1	Shirai
CH^+	0.454 4	2.799	0.02	1	0.0079	−0.5223	Present
22.2	0.103 8	1.161	0.04	0.67	0.14	1.6	Shirai
C^+	0.102 4	1.9178	0.022 96	1.2052	0.0064	−0.4893	Present
22.0	−0.064	1.43	0.013 3	−0.33	0.0424	1.181	Shirai
H_2^+	0.006 3	5.198	0.017 4	−0.7776	0.0272	1.0357	Present
22.3	0.004 9	3.61	0.025 7	−0.039	0.044	1.29	Shirai
H^+	0.049 7	3.5074	0.022 4	−0.8221	0.039	1.035	Present
21.1	0.049 49	2.855	0.031 8	−0.33	0.0513	1.155	Shirai

$$\sigma = \frac{x}{E^2}\left[a_1 \ln x + \sum_{j=2}^{N} a_j \left(1 - \frac{1}{x}\right)^{j-1}\right] 10^{-13}(\text{cm}^2), \qquad (9)$$

where energy E is in eV. They based their analysis on the experimental data of Straub *et al.*[87] and Tian and Vidal,[85] which are slightly higher than recommended data, but the differences are minor. In consequence, the present fits (assuming in principle a ±5% agreement with recommended data) do not differ much from those given by Janev and Reiter,[11] Figs. 18 and 19. Parameters of these fits, together with those obtained by Janev and Reiter are given in Table 15. Rather surprising in these fits are the high values of a_4–a_6 parameters. This reflects numerical difficulties in fitting low energy parts of partial ionization cross sections, for CH_4^+, CH_3^+, H_2^+, and H^+ and would suggest at least two different mechanisms for forming these ions. The problem was studied in detail in coincidence measurements, in particular by Wang and Vidal[92] and Ward *et al.*[89] We discuss their results below.

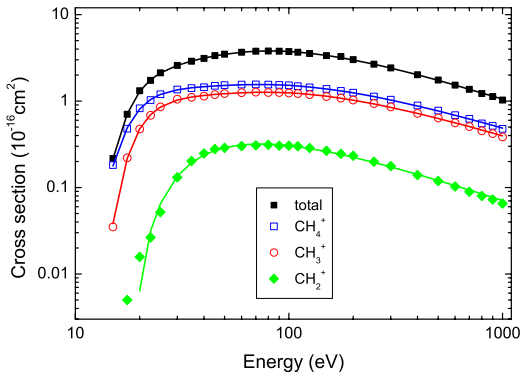

FIG. 18. Approximation of our recommended total and partial ionization cross sections with formula (9) and out fit.

7.2. Semi-empirical estimates and counting ionization cross section

The binary-encounter Bethe–Born (BEB) model developed by Kim *et al.*[93] works well for many atomic, molecular, ionic, and radical targets yielding the total single ionization cross sections within experimental error bars. These targets include H_2, He, Ne, He^+,[93] N_2, H_2O, CO_2, hydrocarbons like C_2H_6, C_3H_8,[93] fluorocarbons,[94] OCS, chlorocarbons (see Vallance *et al.*[83]), and substituted methanes, like CH_2F_2 and CHF_3.[95] However, in case of methane, the BEB model using a vertical ionization potential of 14.25 eV[93] gives a maximum total single ionization cross section of 3.53×10^{-16} cm^2, significantly below all recent measurements, see Figs. 18 and 19. Calculations using a more extensive molecular-orbital base (restricted Hartree–Fock 6–31G++) change these results only slightly—lowering the threshold to 14.13 eV and raising the

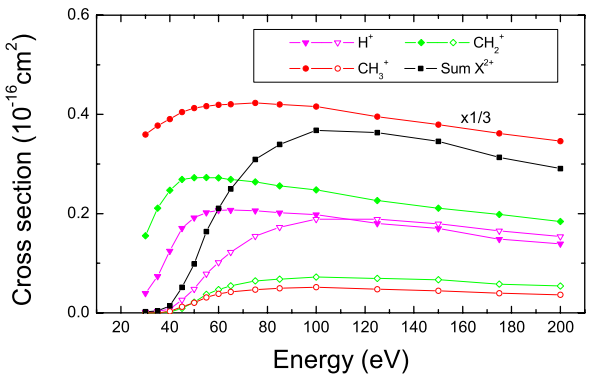

FIG. 19. Multiple ionization in CH_4, selected ions. Closed symbols—single ionization process and open symbols—double ionization precursor (i.e., CH_4^{2+}); relative cross sections from Ward *et al.*,[89] are normalized to our recommended CH_4^+ cross sections.

TABLE 15. Fits to the recommended total and partial ionization cross section using the formula of Janev and Reiter,[11] Eq. (9)

Process threshold (eV)	a_1	a_2	a_3	a_4	a_5	a_6	
Total	2.887 3	−2.257 9	−8.784 2	40.339	−68.811	40.514	Present
12.63	2.344 9	−2.616 3	0.218 4	10.89	−29.718	24.582	Janev
CH_4^+	1.803 4	−1.480 9	−3.828 1	17.892	−30.666	16.38	Present
12.63	1.354 1	−1.466 5	0.167 87	6.180 1	−15.638	10.767	Janev
CH_3^+	1.563 6	−1.376 7	−1.726 2	11.694 8	−23.115 8	13.610 4	Present
12.63	1.607 4	−1.471 3	−0.273 86	0.195 56	0.113 43	0.009 016 6	Janev
CH_2^+	0.213 3	−0.219 4	−0.185 3	0.826 6	−0.139 3	0.004 4	Present
16.2	0.162 5	−0.107 08	−0.322 52	0.871 25	−0.018 747	0.130 71	Janev
CH^+	−0.166 1	0.189 3	−0.388 4	4.061 5	−5.804 5	3.232 4	Present
22.2	−0.124 6	0.162 87	−0.333 95	3.573 8	−5.047 2	2.824	Janev
C^+	−0.123 4	0.036 2	0.552 7	−0.630 3	0.564 8	−0.152 6	Present
22.0	−0.062 13	0.044 75	0.170 5	−0.229 9	0.774 3	−0.290 2	Janev
H_2^+	−0.005 8	0.008 8	−0.077	0.286 5	0.164 4	−0.225 2	Present
22.3	−0.017 61	0.018 35	−0.050 7	0.261 2	0.153 2	−0.173 1	Janev
H^+	−0.431 7	0.351 9	1.479 1	−5.502 1	11.560 4	−4.692 8	Present
21.1	−0.347 0	−0.016 03	4.329 6	−15.155	24.766	−10.873	Janev

maximum to 3.57×10^{-16} cm^2.[95] The model using an adiabatic ionization potential of 12.61 eV[96] gives, in turn, higher results than recent experiments, with a maximum of about 4.3×10^{-16} cm^2. A similar overestimate of the adiabatic ionization potential using BEB is found for NH_3.[93] Therefore, the difference between BEB vertical-potential results and the experiment is probably due the experiment, not the theory. For CF_4, Nishimura *et al.*[94] calculated BEB ionization cross sections using correlated wave functions of the complete-active space (CAS) self-consistent field (SCF) type. This type of wave function allows the effects of multiple ionization to be evaluated. Nishimura *et al.* showed that CAS functions raise the ionization cross sections by about 5% compared to RHF wave functions; this extra 5% represents an estimate of the multiple ionization effect. Wang and Vidal[92] suggested that the difference between BEB and experiments may be due to multiple ionization of CH_4. The analysis is not trivial, as multiple ions were not observed as final products of ionization in methane. However, experimental ionization cross sections for CH_4, independent of the method applied, are to be considered as gross total ionization cross section, which is the total ion current collected, i.e., the charge-weighted sum of partial cross sections,

$$\sigma_{GT} = \sigma_1 + 2\sigma_2 + 3\sigma_3 + \cdots, \tag{10}$$

where σ_i are cross sections for i-fold ionization. The total counting ionization cross section σ_{CT} directly sums the partial cross sections,

$$\sigma_{CT} = \sigma_1 + \sigma_2 + \sigma_3 + \cdots. \tag{11}$$

Formation of unstable dications, CH_4^{2+}, in photoionization of CH_4 has already been observed by Fournier *et al.*[97] According to their measurements, the dication formed from 44 eV photon impact decays preferentially into $(CH_3^+ + H^+)$, $(CH_2^+ + H^+)$, $(CH^+ + H^+)$, and $(CH_2^+ + H_2^+)$ pairs, with the relative branching ratio of 1:0.65:0.15:0.27, respectively. For impact ionization by 200 eV electrons Wang and Vidal[92] stated: "All the alkane dications are unstable and dissociate mostly into ion pairs, in which the production of proton pairs is found to be a major dissociation channel." Gluch *et al.*[86] measured the kinetic energies of ions produced in electron-impact ionization. While CH_4^+ ions appear with only one value of the post-collision kinetic energy, other ions show more complex patterns. In the 28–50 eV energy range, CH_2^+ ions show a growing width of the kinetic energy distribution, and the H^+ ion from threshold clearly shows a double (0.4 and 2.2 eV) distribution of its kinetic energy. This testifies to several distinct processes in which these ions are formed. As noted by Ward *et al.*,[89] these double distributions of the ion kinetic energies would also explain the incomplete collection of ions in the early experiments.[77,78] Ward *et al.*[89] recently measured precursor-specific partial cross sections in the collision energy range of 30–200 eV, using time-of-flight spectroscopy and a two-dimensional coincidence technique. Their data (which must be normalized to the CH_4^+ yield) are in good agreement with the whole series of the recent measurements. The relative amounts of H^+ ions from a single and double ionization at a collision energy of 200 eV scale as 0.111:0.123. Further, in multiple ionization at 200 eV, the dominant dissociation channel of the dication CH_4^{2+} is $(CH_2^+ + H^+ + H)$, followed by $(CH_3^+ + H^+)$ and $(CH^+ + H^+ + 2H)$, with relative intensities of 0.31, 0.25, and 0.16, respectively. The H^+ ion is present as part of an ion pair in 93% of multiple ionization events. Ward *et al.*[89] also confirmed two distinct values of the kinetic energy released in two, $(CH_2^+ + H^+ + H)$ and $(CH^+ + H^+ + H_2)$, of the possible dissociative ionization channels. The above considerations and the unusual shapes of CH_4^+ and CH_3^+ curves, see Fig. 17, which are also confirmed by the values of fitting parameters, allow

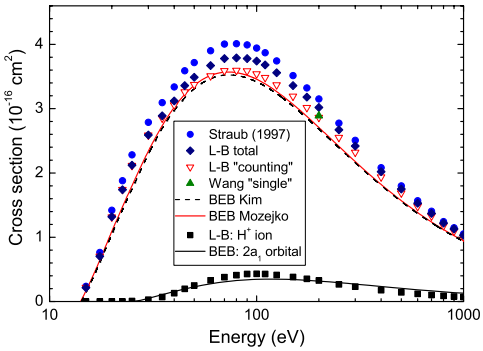

FIG. 20. Tentative evaluation of the total counting (i.e., without multiple counting of dications) cross section in methane. Landolt–Börnstein (L–B) "counting" (open triangles) were obtained by subtracting from L–B recommended data (=sum of all counted ions), diamonds, half of the cross section for H^+ ion yield (squares); the Wang data in the figure are the experimental evaluation of the total single ionization cross section at 200 eV by Wang and Vidal:[92] the BEB data are by Kim *et al.*[93] and Możejko *et al.*[95] vertical ionization potential calculations; the lower continuous line is the BEB calculation[95] for the ionization of the $2a_1$ molecular orbital.

us to evaluate quantitatively the contribution from multiple ionization into the experimental cross sections. Knowing that half of the H^+ ions observed experimentally at 100 eV come from double ionization, we can roughly estimate the counting ionization cross section in methane by subtracting half of the recommended H^+ cross section from the recommended total (=gross) cross section,

$$\sigma_{CT} \approx \sigma_{GT} - 1/2\sigma_{H^+}. \tag{12}$$

The result is shown in Fig. 20. Now, the BEB curve[95] agrees with the recommended experimental values well within the experimental uncertainty. In the same figure, we compare, for sake of illustration merely, the H^+ cross section and the BEB[95] ionization cross section of the molecular $2a_1$ orbital.

In conclusion, Landolt–Börnstein recommended cross section by Lindsay and Mangan[88] is confirmed in the present work by a mutual check of consistency between the experiments, various numerical parameterizations, and BEB theory. In recent measurements,[98] with a quadrupole mass analyzer, dications have been reported, although with very low intensities: CH_4^{2+} at 0.008% relative to CH_4 intensity at 90 eV collision energy and the threshold of 30.5 eV and ($CH_2^{2+} + CH_3^{2+}$) at 0.044% and a 34.5 eV threshold.

8. Dissociation Cross Section

Electron impact dissociation of methane, and other molecules, generally proceeds via electron impact electronic excitation,

$$e + CH_4 \rightarrow e + CH_4^* \rightarrow e + \text{products}. \tag{13}$$

In particular, for methane, all the low-lying electronic states are dissociative so are only very short lived when excited by electron impact. In order of increasing energy threshold, the dissociation products that need to be considered are[99]

$$\begin{aligned} CH_3 + H \quad & \text{(channel 1)}, \\ CH_2 + H_2 \quad & \text{(channel 2)}, \\ CH_2 + 2H \quad & \text{(channel 3)}, \\ CH + H_2 + H \quad & \text{(channel 4)}. \end{aligned} \tag{14}$$

In practice, there are no available measurements that distinguish between channel 2 and channel 3. Furthermore, there are no direct estimates for the dissociation cross sections into channel 4, although Erwin and Kunc[100,101] do present semi-empirical estimates of this quantity. Below, only the total impact dissociation cross section (i.e., sum over all channels), the production of CH_3 (channel 1) and the production of CH_2 (the sum of channels 2 and 3) are considered. Above about 50 eV dissociation into ionic fragments is also possible.[102]

There have been a number of studies on electron impact dissociation of methane.[46,63,72,99–112] These include swarm studies,[45,46,72,103–105] *ab initio* calculations,[63,99,108–110] and semi-empirical studies.[100,101] Fuss *et al.*[1] also present a recommended value for electron impact dissociation stating that it is based on the electron beam measurements of Nakano *et al.*[106] and Makochekanwa *et al.*[112] These measurements are discussed further below, but the values recommended by Fuss *et al.* appear to significantly higher than the published values given in the cited papers. These near-threshold results for electron collision energies up to 15 eV are summarized in Fig. 21. The situation at higher energy is no more straightforward, but there is less primary data to cross-compare.

Early *ab initio* calculations[108–110] did not explicitly consider electron impact dissociation, instead choosing to focus on electron impact electronic excitation. This process is the first step towards dissociation, see Eq. (13). However, these studies only considered a few low-lying states and do not give dissociation cross sections. Since all states of methane are dissociative, electron impact electronic excitation cross sections for individual states are probably not particularly significant and will not be considered here. By far the most comprehensive theoretical treatment of electron impact dissociation of methane is the recent study by Ziółkowski *et al.*[99] This work includes, for the first time for methane or indeed any molecule with more than three atoms, a very detailed treatment of the

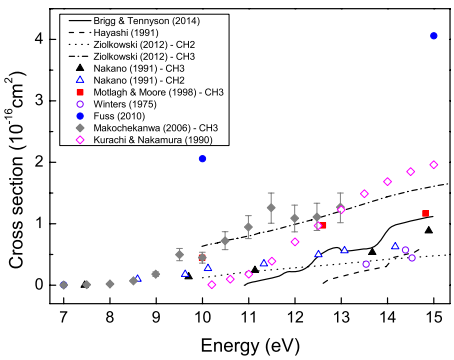

FIG. 21. Electron-impact dissociation cross sections for methane; the values are for total cross sections unless a partial section is given. The data are from beam measurements: Winters,[102] Nakano *et al.*[107] Motlagh and Moore[111] Makochekanwa *et al.*[112] swarm studies: Hayashi[105] Kurachi and Nakamura;[45] *ab initio* calculations Ziółkowski;[99] Brigg *et al.*[63] The recommendations of Fuss *et al.*[1] are also given.

nuclear problem, which allows for the prediction of branching ratios. However, the well-known effect of vibrational motion on the near-threshold dissociation behavior[113] was allowed for only by arbitrarily shifting the dissociation threshold to lower energy. The electron-impact electronic excitation calculations, which were performed with using the R-matrix method as implemented in the UKRMol codes,[114] probably give a lower estimate to the dissociation cross section since only a rather limited representation of the excited target electronic states were included in the calculation. The work of Ziółkowski *et al.*[99] is also the only *ab initio* treatment to give branching ratios. Very recently, Brigg *et al.*[63] completed an R-matrix study also using the UKRMol codes. This work considered a comprehensive set of excited electronic states but only within the fixed nuclei approximation. Since inclusion of nuclear motion can be expected to lead to a significant increase in the dissociation cross section,[113] the cross sections of Brigg *et al.* must also be regarded as an underestimate. Theoretically, what is required is a combination of the comprehensive treatment of electronic states, as performed by Brigg *et al.*, inclusion of nuclear motion after excitation, and the careful treatment of nuclear motion along the lines of Ziółkowski *et al.*[99] for branching ratios. However, such a study would be extremely computationally demanding.

TABLE 16. Recommended dissociative attachment cross sections (CS) for the formation of H^- and CH_2^-, and total dissociative electron attachment cross section from methane in the units of 10^{-18} cm^2, electron energies are in eV

Energy	H^- CS	CH_2^- CS	Total CS	Energy	H^- CS	CH_2^- CS	Total CS	Energy	H^- CS	CH_2^- CS	Total CS
6	0.015 15	0.016 36	0.031 51	10.5	1.378 49	0.128 45	1.506 94	15	0.035 6	0.014 43	0.050 03
6.1	0.012 62	0.012 99	0.025 61	10.6	1.424 08	0.131 34	1.555 43	15.1	0.015 14	0.020 21	0.035 35
6.2	0.024 77	0.007 7	0.032 47	10.7	1.312 77	0.112 58	1.425 34	15.2	0.033 09	0.019 24	0.052 33
6.3	0.038 86	0.007 7	0.046 55	10.8	1.280 86	0.121 24	1.402 1	15.3	0.039 18	0.014 43	0.053 61
6.4	0.040 24	0.009 62	0.049 86	10.9	1.196 91	0.110 65	1.307 56	15.4	0.015 95	0.018 76	0.034 71
6.5	0.071 32	0.008 66	0.079 98	11	1.024 92	0.105 36	1.130 28	15.5	0.016 36	0.018 76	0.035 12
6.6	0.039 6	0.006 74	0.046 34	11.1	1.076 03	0.100 07	1.176 1	15.6	0.036 27	0.024 05	0.060 32
6.7	0.031 03	0.013 95	0.044 98	11.2	0.963 3	0.099 11	1.062 4	15.7	0.026 71	0.015 88	0.042 59
6.8	0.082	0.012 03	0.094 03	11.3	0.910 81	0.089	0.999 81	15.8	0.026 79	0.027 9	0.054 69
6.9	0.102 03	0.010 1	0.112 13	11.4	0.774 08	0.077 46	0.851 54	15.9	0.045 85	0.021 17	0.067 02
7	0.070 91	0.004 33	0.075 24	11.5	0.717 28	0.093 33	0.810 61	16	0.038 22	0.025 98	0.0642
7.1	0.006 72	0.010 1	0.016 82	11.6	0.660 71	0.074 09	0.734 8	16.1	0.026 97	0.020 69	0.047 65
7.2	0.079 84	0.011 07	0.090 91	11.7	0.521 38	0.063 99	0.585 36	16.2	0.048 49	0.022 61	0.071 1
7.3	0.084 78	0.008 18	0.092 95	11.8	0.504 81	0.063 99	0.568 8	16.3	0.057 84	0.022 13	0.079 97
7.4	0.124 06	0.012 03	0.136 08	11.9	0.468 47	0.056 29	0.524 76	16.4	0.030 36	0.025 5	0.055 86
7.5	0.159 63	0.011 55	0.171 17	12	0.396 92	0.046 19	0.443 11	16.5	0.027 21	0.028 38	0.055 59
7.6	0.254 69	0.015 4	0.270 09	12.1	0.324 22	0.052 44	0.376 66	16.6	0.040 91	0.029 83	0.070 74
7.7	0.262 31	0.015 88	0.278 19	12.2	0.315 96	0.043 3	0.359 26	16.7	0.027 02	0.023 09	0.050 11
7.8	0.383 7	0.013 95	0.397 65	12.3	0.241 73	0.037 04	0.278 77	16.8	0.050 08	0.022 61	0.072 69
7.9	0.380 49	0.015 88	0.396 37	12.4	0.241 97	0.032 23	0.274 2	16.9	0.038 76	0.024 05	0.062 81
8	0.569 51	0.010 58	0.580 09	12.5	0.205 03	0.032 71	0.237 74	17	0.040 35	0.030 31	0.070 66
8.1	0.643 72	0.020 69	0.664 41	12.6	0.184 12	0.030 31	0.214 43	17.1	0.039 4	0.030 79	0.070 19
8.2	0.699 02	0.025 5	0.724 52	12.7	0.142 38	0.025 98	0.168 36	17.2	0.035 65	0.030 31	0.065 96
8.3	0.889 81	0.018 28	0.908 09	12.8	0.142 17	0.031 27	0.173 44	17.3	0.045 23	0.028 38	0.073 61
8.4	0.942 55	0.027 42	0.969 97	12.9	0.145 13	0.021 65	0.166 78	17.4	0.088 22	0.018 76	0.106 99
8.5	1.104 19	0.025 5	1.129 69	13	0.113 87	0.025 02	0.138 89	17.5	0.055 16	0.029 83	0.084 99
8.6	1.191 85	0.022 61	1.214 46	13.1	0.087 86	0.017 32	0.105 18	17.6	0.059 41	0.028 38	0.087 8
8.7	1.255 98	0.030 79	1.286 77	13.2	0.086 01	0.020 69	0.106 69	17.7	0.050 44	0.031 27	0.081 71
8.8	1.236 61	0.024 05	1.260 66	13.3	0.055 42	0.017 32	0.072 74	17.8	0.071 99	0.032 23	0.104 23
8.9	1.258 61	0.031 75	1.290 37	13.4	0.070 95	0.020 69	0.091 64	17.9	0.067 42	0.027 9	0.095 32
9	1.416 09	0.029 35	1.445 43	13.5	0.040 42	0.019 73	0.060 14	18	0.041 79	0.031 27	0.073 06
9.1	1.416 46	0.031 27	1.447 73	13.6	0.055 82	0.014 91	0.070 74	18.1	0.057 02	0.028 87	0.085 89
9.2	1.488 83	0.040 41	1.529 24	13.7	0.042 84	0.012 99	0.055 83	18.2	0.077 23	0.036 08	0.113 31
9.3	1.480 53	0.048 11	1.528 64	13.8	0.031 66	0.012 03	0.043 69	18.3	0.089 44	0.036 56	0.126 01
9.4	1.588 23	0.065 43	1.653 66	13.9	0.049 48	0.015 88	0.065 36	18.4	0.051 34	0.031 75	0.083 09
9.5	1.564 48	0.080 34	1.644 82	14	0.032 72	0.022 13	0.054 85	18.5	0.111 11	0.034 16	0.145 26
9.6	1.536 55	0.082 75	1.619 3	14.1	0.043 54	0.016 36	0.059 9	18.6	0.108 29	0.033 2	0.141 48
9.7	1.592 93	0.084 67	1.677 61	14.2	0.029 72	0.016 36	0.046 07	18.7	0.111 77	0.030 79	0.142 56
9.8	1.516 13	0.095 26	1.611 38	14.3	0.039 2	0.017 8	0.057	18.8	0.055 91	0.035 12	0.091 03
9.9	1.584 7	0.100 55	1.685 25	14.4	0.024 06	0.019 24	0.043 31	18.9	0.072 3	0.040 41	0.112 71
10	1.510 22	0.122 68	1.632 9	14.5	0.032 87	0.018 28	0.051 15	19	0.087 44	0.031 27	0.118 71
10.1	1.520 8	0.124 12	1.644 92	14.6	0.022 16	0.015 88	0.038 04	19.1	0.107 23	0.037 53	0.144 75
10.2	1.458 21	0.132 3	1.590 51	14.7	0.038 18	0.013 95	0.052 13	19.2	0.117 73	0.038 97	0.1567
10.3	1.497 63	0.130 86	1.628 49	14.8	0.038 68	0.021 65	0.060 33	19.3	0.142 43	0.031 27	0.173 7
10.4	1.402 69	0.14	1.542 69	14.9	0.038 45	0.018 76	0.057 21	19.4	0.154 22	0.035 12	0.189 34

Recent beam measurements include those of described by Nakano *et al.*,[107] who considered fragmentation into both CH_3 and CH_2, and Makochekanwa *et al.*,[112] who only considered fragmentation to the CH_3 channel. Unfortunately, the results of the two studies are incompatible since the one-channel cross sections of Makochekanwa *et al.*[112] are significantly larger than the two channel ones of Nakano *et al.* At this time, it is not possible to make a clear recommendation for either total or partial electron-impact dissociation cross sections for methane. This problem, which is important for a number of topics including plasma-aided combustion, clearly requires further study.

9. DEA Cross Section

In 1967, Sharp and Dowell[115] measured the total attachment cross section using the total ionization method and normalized their data to the positive ion cross section. The cross section curve showed two peaks. They assigned the low-energy peak as the production of H^- and the high-energy peak as CH_2^-. There is no mention of uncertainty. In 2008, Rawat *et al.*[116] measured the absolute cross sections for the formation of H^- and CH_2^- from methane, with special care to eliminate discrimination due to kinetic energy and angular distribution of the fragment ions. The overall uncertainty in these measurements was estimated to be a maximum of ±15%. There is a huge difference between Rawat *et al.* and Sharp and Dowell in the total attachment cross section. Rawat *et al.* noted that H^- and CH_2^- are the dominant channels, though due to limited mass resolution, we cannot rule out the presence of CH^-. The total dissociative electron attachment (DEA) cross section at the resonant peak of 9.9 eV was found to be 1.7×10^{-18} cm^2. In 2011, Hoshino *et al.*[117] reported relative results for C^-, CH^-, CH_2^-, and CH_3^- anions formed from DEA to CH_4. The CH_2^- anion was observed to be the most abundant species produced from the dissociative electron attachment of CH_4, and the resonance feature peaks at 10.3 eV. CH^- is the next in magnitude, showing a resonance peak at 10.8 eV, and is much weaker and narrower than CH_2^-. Peak positions of CH_2^- of Sharp and Dowell, Rawat *et al.*, and Hoshino *et al.* agree very well.

We recommend the data of Rawat *et al.*,[116] because (1) they are much more recent and used a more advanced apparatus compared to the experiment of Sharp and Dowell and (2) Rawat *et al.* reported uncertainty, while Sharp and Dowell[115] did not. The recommended cross sections are given in Table 16 and Fig. 22.

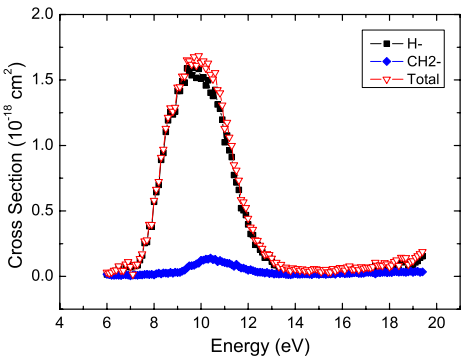

FIG. 22. Recommended cross sections for the formation of H^- and CH_2^- and total dissociative electron attachment cross section from methane.

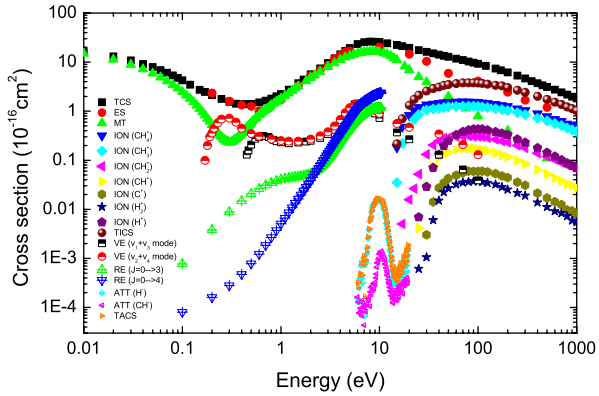

FIG. 23. The summary of cross section for electron collisions with methane. TCS - total scattering, ES - elastic scattering, MT - momentum transfer, ION - partial ionization, TICS - total ionization, VE - vibrational excitation, RE - rotational excitation, ATT - dissociative attachment, and TACS - total dissociative attachment.

10. Summary and Future Work

We present a systematic review of the published cross sections for processes resulting from electron collisions with methane up to early 2014. Both measurements and theoretical predictions are considered, although priority is given to high quality measurements with published uncertainties where available. The summary of cross section for electron collisions with methane are given in Fig. 23.

There is considerable variation in the reliability of the available data. For the total cross section, the momentum transfer cross section and the ionization cross section, it is possible to recommend values over an extended energy range with small uncertainties, typically 5%–10%. The situation is less satisfactory for other processes. For electron impact rotational excitation, we rely on predictions from *ab initial* calculations. Because of the high symmetry of methane, these cross sections are small and hard to determine empirically but experimental work on this process would be welcome. There are only very limited number of direct experimental measurements of electron impact vibrational excitation cross sections, and the data do not agree well with each other. The more extensive theoretical treatments of this process do not give results which agree with cross sections determined from swarm experiments. We recommend the vibrational excitation cross sections determined from swarm measurements but note that this is only and indirect measurement for which it is hard to establish true uncertainties. Some new, reliable beam measurements of this process would be very helpful. Electron impact dissociation of methane is an important process but the available measurements are inconsistent with each other, and we are unable to recommend a good set of data for this process. A new study on the problem is needed. Finally, there are only sparse data available for the dissociative electron attachment process:

Here, we recommend using the most recent experimental data but are not able to provide estimated uncertainties.

This evaluation is the first in series of systematic evaluations of electron collision processes for key molecular targets. Other evaluations will appear in future papers.

Acknowledgments

This work was partial supported by the Degree & Research Center Program of the Korea Research Council of Fundamental Science and Technology and Ministry of Trade, Industry and Energy through Standard Reference Data Program. We appreciate help of Dr. A. Karbowski in the numerical analysis of the ionization cross sections. One of us (G.K.) acknowledges greatly the hospitality at Data Center for Plasma Properties, NFRI, Gunsan. H.C. acknowledges the support from the National Fusion Research Institute and the National Research Foundation, Korea (Grant No. 2010-0021120). V.K. acknowledges partial support from the National Science Foundation, Grant No. PHY-10-68785.

11. References

[1]M. C. Fuss, A. Munõz, J. C. Oller, F. Blanco, M.-J. Hubin-Franskin, D. Almeida, P. Limão-Vieira, and G. García, Chem. Phys. Lett. **486**, 110 (2010).
[2]M. Cascella, R. Čurik, and F. A. Gianturco, J. Phys. B: At. Mol. Opt. Phys. **34**, 705 (2001).
[3]L. D. Horton, Phys. Scr. **T65**, 175 (1996).
[4]N. L. Aleksandrov, S. V. Kindysheva, E. N. Kukaev, S. Starikovskaya, and A. Y. Starikovskii, Plasma Phys. Rep. **35**, 867 (2009).
[5]J. Tauer, H. Kofler, and E. Winter, Laser Photonics Rev. **4**, 99 (2009).
[6]E. H. Wilson and S. K. Atreya, J. Geophys. Res. **109**, E06002 (2004).
[7]W. L. Morgan, Plasma Chem. Plasma Process. **12**, 477 (1992).
[8]I. Kanik, S. Trajmar, and J. C. Nickel, J. Geophys. Res. **98**, 7447 (1993).
[9]G. P. Karwasz, R. S. Brusa, and A. Zecca, La Rivista del Nuovo Cimento **24**, 1 (2001).
[10]T. Shirai, T. Tabata, H. Tawara, and Y. Itikawa, At. Data Nucl. Data Tables **80**, 147 (2002).
[11]R. K. Janev and D. Reiter, Phys. Plasmas **9**, 4071 (2002).
[12]J. Ferch, B. Granitza, and W. Raith, J. Phys. B: At. Mol. Opt. Phys. **18**, L445 (1985).
[13]B. Lohmann and S. J. Buckman, J. Phys. B: At. Mol. Opt. Phys. **19**, 2565 (1986).
[14]R. K. Jones, J. Chem. Phys. **82**, 5424 (1985).
[15]A. Zecca, G. Karwasz, R. S. Brusa, and C. Szmytkowski, J. Phys. B: At. Mol. Opt. Phys. **24**, 2747 (1991).
[16]M. S. Dababneh, Y.-F. Hsieh, W. E. Kaupilla, C. K. Kwan, S. J. Smith, T. S. Stein, and M. N. Uddin, Phys. Rev. A **38**, 1207 (1988).
[17]H. Nishimura and T. Sakae, Jpn. J. Appl. Phys., Part 1 **29**, 1372 (1990).
[18]I. Kanik, S. Trajmar, and J. C. Nickel, Chem. Phys. Lett. **193**, 281 (1992).
[19]W. M. Ariyasinghe, T. Wijeratne, and P. Palihawadana, Nucl. Instrum. Methods Phys. Res., Sect. B **217**, 389 (2004).
[20]G. García and F. Manero, Phys. Rev. A **57**, 1069 (1998).
[21]E. Barbarito, M. Basta, M. Calicchio, and G. Tessari, J. Chem. Phys. **71**, 54 (1979).
[22]O. Sueoka and S. Mori, J. Phys. B: At. Mol. Opt. Phys. **19**, 4035 (1986).
[23]K. Floeder, D. Fromme, W. Raith, A. Schwab, and G. Sinapius, J. Phys. B: At. Mol. Opt. Phys. **18**, 3347 (1985).
[24]G. P. Karwasz, R. S. Brusa, and A. Zecca, in *Landolt-Börnstein: Numerical Data Functional Relationships in Science and Technology. New Series, Group I: Elementary Particles Nuclei and Atoms. Volume 17, Photon and Electron Interactions with Atoms, Molecules and Ions. Subvolume C, Interactions of Photons and Electrons with Molecules*, edited by W. Martienssen (Springer, Berlin, Heidelberg, New York, 2003).
[25]K. Fedus and G. P. Karwasz, Eur. Phys. J. D **68**, 93 (2014).
[26]M. Allan, J. Phys. B: At. Mol. Opt. Phys. **38**, 1679 (2005).
[27]A. Zecca, G. P. Karwasz, and R. S. Brusa, J. Phys. B: At. Mol. Opt. Phys. **33**, 843 (2000).
[28]A. Zecca, I. Lazzizzera, M. Krauss, and C. E. Kuyatt, J. Chem. Phys. **61**, 4560 (1974).
[29]O. Sueoka, S. Mori, and Y. Katayama, J. Phys. B: At. Mol. Opt. Phys. **19**, L373 (1986).
[30]O. Sueoka, S. Mori, and Y. Katayama, J. Phys. B: At. Mol. Opt. Phys. **20**, 3237 (1987).
[31]C. Ramsauer and R. Kollath, Ann. Phys. (Leipzig) **4**, 91 (1930).
[32]E. Brüche, Ann. Phys. (Leipzig) **83**, 1065 (1927).
[33]E. Brüche, Ann. Phys. (Leipzig) **84**, 387 (1930).
[34]R. B. Brode, Phys. Rev. **25**, 636 (1925).
[35]M. Allan, AIP Conf. Proc. **901**, 107 (2007).
[36]L. Boesten and H. Tanaka, J. Phys. B: At., Mol. Opt. Phys. **24**, 821 (1991).
[37]C. T. Bundschu, J. C. Gibson, R. J. Gulley, M. J. Brunger, S. J. Buckman, N. Sanna, and F. A. Gianturco, J. Phys. B: At., Mol. Opt. Phys. **30**, 2239 (1997).
[38]H. Cho, Y. S. Park, E. A. Y. Castro, G. de Souza, I. Iga, L. E. Machado, L. M. Brescansin, and M.-T. Lee, J. Phys. B: At., Mol. Opt. Phys. **41**, 045203 (2008).
[39]I. I. Iga, M.-T. Lee, M. Homen, L. E. Machado, and L. M. Brescansin, Phys. Rev. A **61**, 022708 (2000).
[40]T. Sakae, S. Sumiyoshi, E. Murakami, Y. Matsumoto, K. Ishibashi, and A. Katase, J. Phys. B: At., Mol. Opt. Phys. **22**, 1385 (1989).
[41]T. W. Shyn and T. E. Cravens, J. Phys. B: At., Mol. Opt. Phys. **23**, 293 (1990).
[42]W. Sohn, K.-H. Kochem, K.-M. Scheuerlein, K. Jung, and H. Ehrhardt, J. Phys. B: At., Mol. Opt. Phys. **19**, 3625 (1986).
[43]H. Tanaka, T. Okada, L. Boesten, T. Suzuki, T. Yamamoto, and M. Kubo, J. Phys. B: At. Mol. Opt. Phys. **15**, 3305 (1982).
[44]E. A. Y. Castro, G. L. C. Souza, L. M. Brescansin, L. E. Machado, A. S. dos Santos, and M.-T. Lee, J. Electron Spectrosc. Relat. Phenom. **182**, 4 (2010).
[45]M. Kurachi and Y. Nakamura, *Proceedings of 13th Symposium on Ion Sources and Ion-Assisted Technology*, edited by T. Takagi (Tokyo, 1990), p. 205.
[46]D. K. Davies, L. E. Kline, and W. E. Bies, J. Appl. Phys. **65**, 3311 (1989).
[47]G. N. Haddad, Aust. J. Phys. **38**, 677 (1985).
[48]N. Gee and G. R. Freeman, Phys. Rev. A **20**, 1152 (1979).
[49]H. Alvarez-Pol, I. Duran, and R. Lorenzo, J. Phys. B: At. Mol. Opt. Phys. **30**, 2455 (1997).
[50]B. Schmidt, J. Phys. B: At. Mol. Opt. Phys. **24**, 4809 (1991).
[51]S. Pancheshnyi, S. Biagi, M. C. Bordage, G. J. M. Hagelaar, W. L. Morgan, A. V. Phelps, and L. C. Pitchford, Chem. Phys. **398**, 148 (2012).
[52]R. Müller, K. Jung, K.-H. Kochem, W. Sohn, and H. Ehrhardt, J. Phys. B: At. Mol. Opt. Phys. **18**, 3971 (1985).
[53]L. Vušković and S. Trajmar, J. Chem. Phys. **78**, 4947 (1983).
[54]M. Brunger, S. J. Buckman, and M. T. Elford, in *Landolt-Börnstein: Numerical data Functional Relationships in Science and Technology. New Series, Group I: Elementary Particles Nuclei and Atoms. Volume 17, Photon and Electron Interactions with Atoms, Molecules and Ions. Subvolume C, Interactions of Photons and Electrons with Molecules*, edited by W. Martienssen (Springer, Berlin, Heidelberg, New York, 2003), p. 6118.
[55]T. K. Bose, J. S. Sochanski, and R. H. Cole, J. Chem. Phys. **57**, 3592 (1972).
[56]Y. Itikawa and N. Mason, Phys. Rep. **414**, 1 (2005).
[57]N. Abusalbi, R. A. Eades, T. Nam, D. Thirumalai, D. A. Dixon, D. G. Truhlar, and M. Dupuis, J. Chem. Phys. **78**, 1213 (1983).
[58]F. A. Gianturco, A. Jain, and L. C. Pantano, J. Phys. B: At. Mol. Opt. Phys. **20**, 571 (1987).
[59]P. McNaughten, D. G. Thompson, and A. Jain, J. Phys. B: At. Mol. Opt. Phys. **23**, 2405S (1990).
[60]L. M. Brescansin, M. A. P. Lima, and V. McKoy, Phys. Rev. A **40**, 5577 (1989).
[61]M. T. do N. Varella, M. H. F. Bettega, and M. A. P. Lima, Z. Phys. D: At., Mol. Clusters **39**, 59 (1997).
[62]L. E. Machado, L. M. Brescansin, and M.-T. Lee, Braz. J. Phys. **32**, 804 (2002).
[63]W. J. Brigg, J. Tennyson, and M. Plummer, J. Phys. B: At., Mol. Opt. Phys. **47**, 185203 (2014).
[64]H. Tanaka, M. Kubo, N. Onodera, and A. Suzuki, J. Phys. B: At., Mol. Opt. Phys. **16**, 2861 (1983).
[65]T. Shyn, J. Phys. B: At., Mol. Opt. Phys. **24**, 5169 (1991).
[66]R. Čurik, P. Čársky, and M. Allan, J. Phys. B: At., Mol. Opt. Phys. **41**, 115203 (2008).

[67]S. Althorpe, F. Gianturco, and N. Sanna, J. Phys. B: At., Mol. Opt. Phys. **28**, 4165 (1995).
[68]H. Tawara, Y. Itikawa, H. Nishimura, H. Tanaka, and Y. Nakamura, NIFS-DATA-6, 1990.
[69]Y. Nakamura, The Papers of Technical Meeting on Electrical Discharges, IEE Japan, ED-84-28, 1984.
[70]S. Obata, M. Komada, and Y. Nakamura, The Papers of Technical Meeting on Electrical Discharges, IEE Japan, ED-89-71, 1989.
[71]K. F. Ness and R. E. Robson, Phys. Rev. A **34**, 2185 (1986).
[72]S. R. Hunter, J. G. Carter, and L. G. Christophorou, J. Appl. Phys. **60**, 24 (1986).
[73]B. Schmidt and M. Roncossek, Aust. J. Phys. **45**, 351 (1992).
[74]J. de Urquijo, I. Alvarez, E. Basurto, and C. Cisneros, J. Phys. D: Appl. Phys. **32**, 1646 (1999).
[75]L. Hughes and E. Klein, Phys. Rev. **23**, 450 (1924).
[76]D. Rapp and P. Englander-Golden, J. Chem. Phys. **43**, 1464 (1965).
[77]B. Adamczyk, A. J. H. Boerboom, B. L. Schram, and J. Kistemaker, J. Chem. Phys. **44**, 4640 (1966).
[78]H. Chatham, D. Hills, R. Robertson, and A. Gallagher, J. Chem. Phys. **81**, 1770 (1984).
[79]N. Djurić, I. Cadez, and M. Kurepa, Int. J. Mass Spectrom. Ion Processes **108**, R1 (1991).
[80]H. Nishimura and H. Tawara, J. Phys. B: At. Mol. Opt. Phys. **27**, 2063 (1994).
[81]H. C. Straub, P. Renault, B. G. Lindsay, K. A. Smith, and R. F. Stabbings, Phys. Rev. A **52**, 1135 (1995).
[82]V. Tarnovsky, A. Levin, H. Deutsch, and K. Becker, J. Phys. B: At. Mol. Opt. Phys. **29**, 139 (1996).
[83]C. Vallance, S. A. Harris, J. E. Hudson, and P. W. Harland, J. Phys. B: At. Mol. Opt. Phys. **30**, 2465 (1997).
[84]C. C. Tian and C. R. Vidal, Chem. Phys. **222**, 105 (1997).
[85]C. C. Tian and C. R. Vidal, J. Phys. B: At. Mol. Opt. Phys. **31**, 895 (1998).
[86]K. Gluch, P. Scheier, W. Schustereder, T. Tepnual, L. Feketeova, C. Mair, S. Matt-Leubner, A. Stamatovic, and T. D. Mark, Int. J. Mass Spectrom. **228**, 307 (2003).
[87]C. Straub, D. Lin, B. G. Lindsay, K. A. Smith, and R. F. Stebbings, J. Chem. Phys. **106**, 4430 (1997).
[88]B. G. Lindsay and M. A. Mangan, in *Landolt-Börnstein: Numerical Data and Functional Relationships in Science and Technology. New Series, Group I: Elementary Particles, Nuclei and Atoms. Volume 17, Photon and Electron Interactions with Atoms, Molecules and Ions. Subvolume C, Interactions of Phtotons and Electrons with Molecules*, edited by W. Martienssen (Springer, Berlin, Heidelberg, New York, 2003), p. 5001.
[89]M. D. Ward, S. J. King, and S. D. Price, J. Chem. Phys. **134**, 024398 (2011).
[90]O. J. Orient and S. K. Srivastava, J. Phys. B: At. Mol. Opt. Phys. **20**, 3923 (1987).
[91]V. Dose, P. Pecher, and R. Preuss, J. Phys. Chem. Ref. Data **29**, 1157 (2000).
[92]P. Q. Wang and C. R. Vidal, Chem. Phys. **280**, 309 (2002).
[93]Y. K. Kim, W. Hwang, N. M. Weinberger, M. A. Ali, and M. E. Rudd, J. Chem. Phys. **106**, 1026 (1997).
[94]H. Nishimura, W. M. Huo, M. A. Ali, and Y.-K. Kim, J. Chem. Phys. **110**, 3811 (1999).
[95]G. P. Karwasz, P. Możejko, and M.-Y. Song, Int. J. Mass Spectrom. **365-366**, 232 (2013).
[96]W. Hwang, Y.-K. Kim, and M. E. Rudd, J. Chem. Phys. **104**, 2956 (1996).
[97]P. G. Fournier, J. Fournier, F. Salama, P. J. Richardson, and J. H. D. Eland, J. Chem. Phys. **83**, 241 (1985).
[98]A. N. Zavilopulo, M. I. Mykyta, and O. R. Shpenik, Tech. Phys. Lett. **38**, 947 (2012) [Pisma v Zhurnal Tekhnicheskoi Fiziki **38**, 69 (2012)].
[99]M. Ziółkowski, A. Vikar, M. L. Mayes, A. Bencsura, G. Lendvay, and G. C. Schatz, J. Chem. Phys. **137**, 22A510 (2012).
[100]D. A. Erwin and J. A. Kunc, Phys. Rev. A **72**, 052719 (2005).
[101]D. A. Erwin and J. A. Kunc, J. Appl. Phys. **103**, 064906 (2008).
[102]H. F. Winters, J. Chem. Phys. **63**, 3462 (1975).
[103]N. Goto and T. Makabe, J. Phys. D: Appl. Phys. **23**, 686 (1990).
[104]Y. Ohmori, K. Kitamori, M. Shimozuma, and H. Tagashira, J. Phys. D: Appl. Phys. **19**, 437 (1986).
[105]M. Hayashi, *Electron Collision Cross-Sections Determined from Beam and Swarm Data by Boltzmann Analysis*, NATO ASI, Vol. 220 (Plenum, New York, 1991), pp. 333–340.
[106]T. Nakano, H. Toyoda, and H. Sugai, Jpn. J. Appl. Phys., Part 1 **30**, 2912 (1991).
[107]T. Nakano, H. Toyoda, and H. Sugai, Jpn. J. Appl. Phys., Part 1 **30**, 2908 (1991).
[108]C. Winstead, Q. Sun, V. McKoy, J. L. S. Lino, and M. A. P. Lima, J. Chem. Phys. **98**, 2132 (1993).
[109]T. J. Gil, B. H. Lengsfield, C. W. McCurdy, and T. N. Rescigno, Phys. Rev. A **49**, 2551 (1994).
[110]M. Bettega, L. Ferreira, and M. Lima, Phys. Rev. A **57**, 4987 (1998).
[111]S. Motlagh and J. H. Moore, J. Chem. Phys. **109**, 432 (1998).
[112]C. Makochekanwa, K. Oguri, R. Suzuki, T. Ishihara, M. Hoshino, M. Kimura, and H. Tanaka, Phys. Rev. A **74**, 042704 (2006).
[113]D. T. Stibbe and J. Tennyson, New J. Phys. **1**, 2 (1998).
[114]J. M. Carr, P. G. Galiatsatos, J. D. Gorfinkiel, A. G. Harvey, M. A. Lysaght, D. Madden, Z. Masin, M. Plummer, and J. Tennyson, Eur. Phys. J. D **66**, 58 (2012).
[115]T. E. Sharp and J. T. Dowell, J. Chem. Phys. **46**, 1530 (1967).
[116]P. Rawat, V. Prabhudesai, M. A. Rahman, N. Bhargava Ram, and E. Krishnakumar, Int. J. Mass Spectrom. **277**, 96 (2008).
[117]M. Hoshino, S. Matejcik, Y. Nunes, F. Ferreira da Silva, P. Limao-Vieira, and H. Tanaka, Int. J. Mass Spectrom. **306**, 51 (2011).